https://youtu.be/jNZmrQz0b4g

Electron Screening in Palladium

Matej Lipoglavšek

Jožef Stefan Institute, Ljubljana, Slovenia

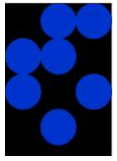

Russbach, March 2023

Astrophysical S-factor

$$\sigma(E) = \frac{S(E)}{E} e^{-2\pi\eta},$$

σ - cross section,
S(E) – S factor,
E – geometrical factor,
$e^{-2\pi\eta}$ - Gamow factor.

^{7}Li(p,α)^{4}He Cross Section

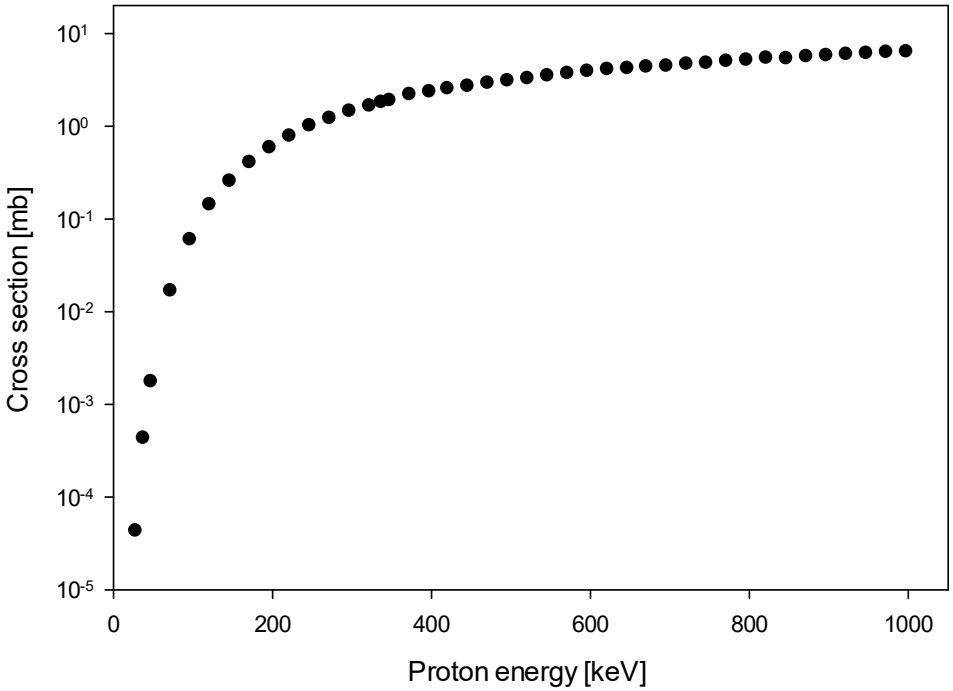

C. Rolfs and R.W.Kavanagh, Nucl. Phys. **A455** (1986) 179.

Tunneling

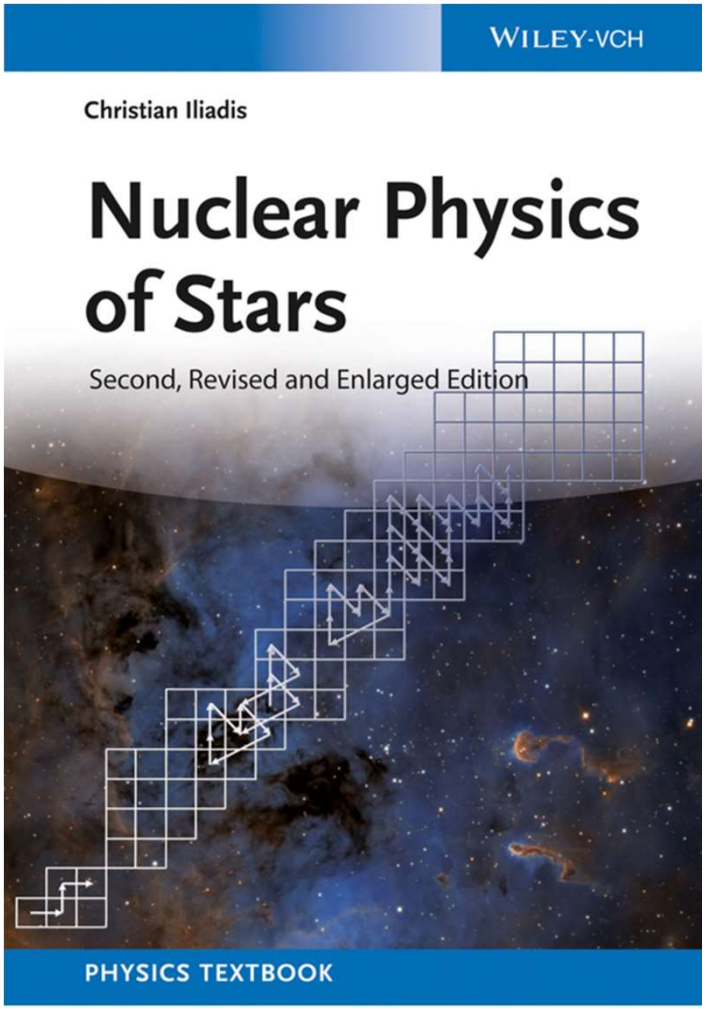

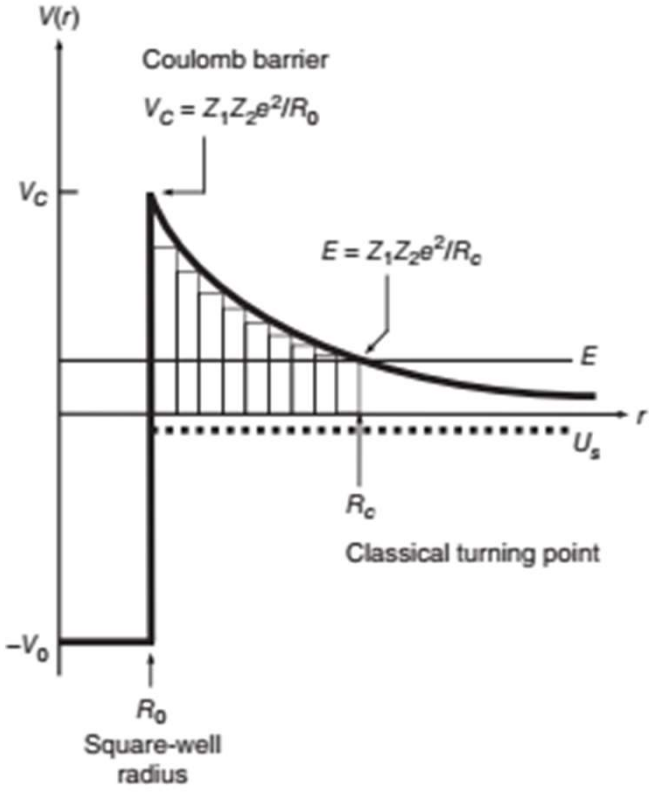

Coulomb barrier transmission probability

$T = e^{-2\pi\eta}$, Gamow factor, where

Sommerfeld parameter: $\eta = \frac{Z_1 Z_2 e^2}{4\pi\varepsilon_0 \hbar c} \cdot \sqrt{\frac{\mu c^2}{2E}}$

Electron Screening

Cross section increases at low energies when the interacting nuclei are not bare. Enhancement factor

$$f = \frac{e^{-2\pi\eta(E+Ue)}}{e^{-2\pi\eta(E)}}$$

where U_e is the screeening potential.

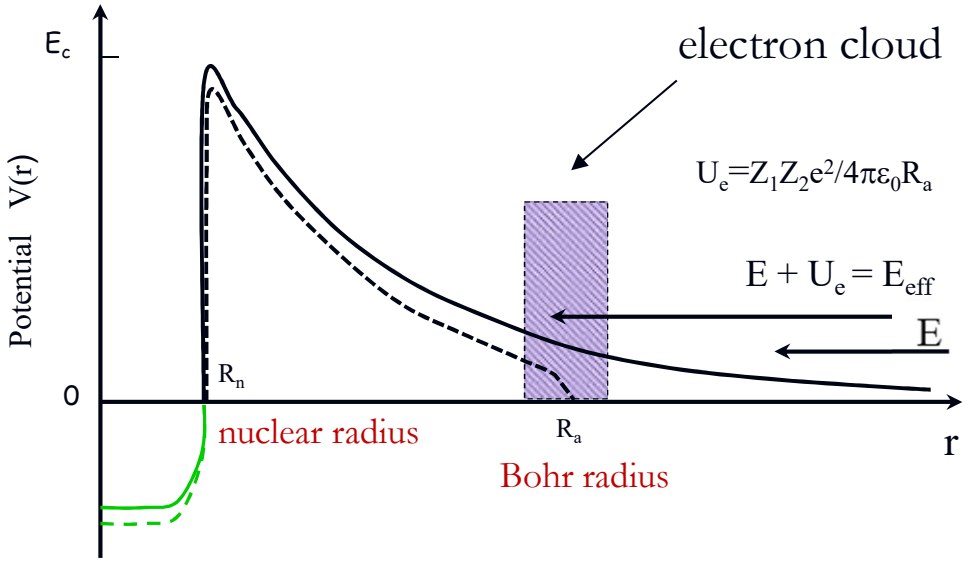

H. J. Assenbaum, K. Langanke and C. Rolfs, Z. Phys. A **327** (1987) 461.
395 citations (Web of Science, November 2021).

$$\frac{R_n}{R_a} \approx 10^{-5} \Rightarrow U_e = \frac{e^2}{4\pi\varepsilon_0 R_a} = 27 \text{ eV for d+d reaction}$$

Previous Results 1

for d(d,p)t reaction from F. Raiola et al., Eur. Phys. J. A**19** (2004) 283.

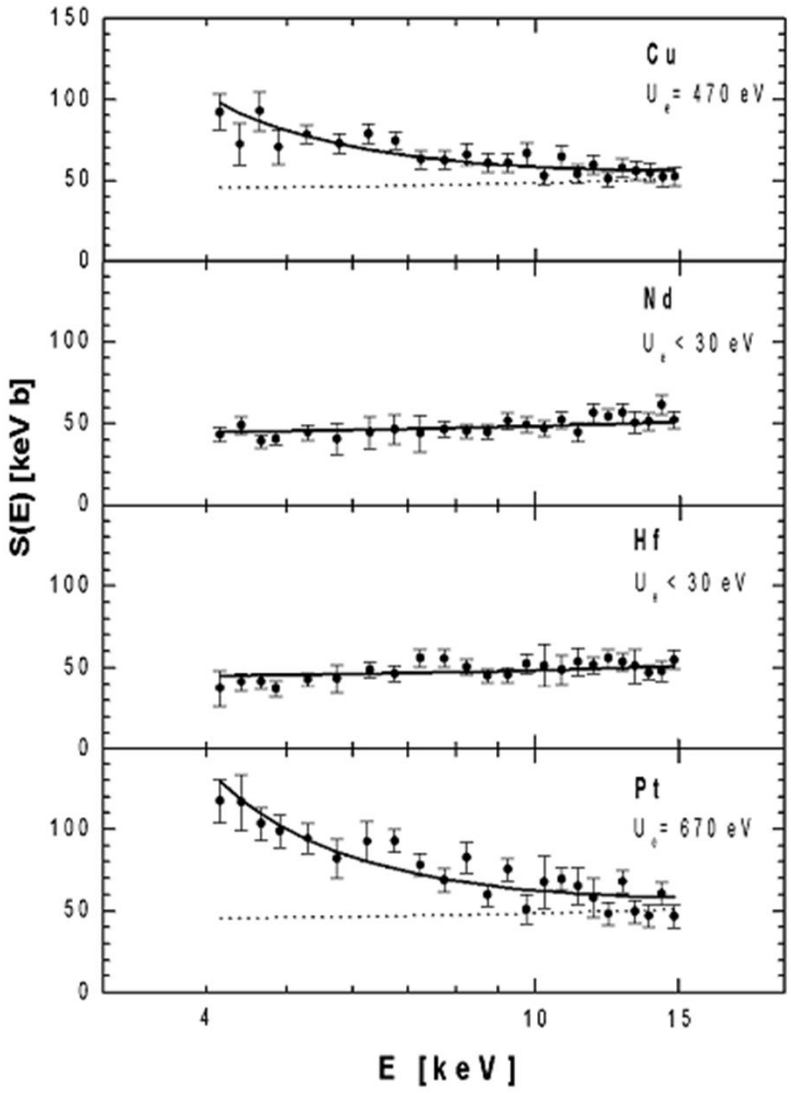

Material	U_e (eV)[b]	Solubility $1/x$ [c]	n_{eff} [b]	n_{eff} (Hall)[d]
		Metals		
Be	180±40	0.08	0.2±0.1	(0.21±0.04)
Mg	440±40	0.11	3.0±0.5	1.8±0.4
Al	520±50	0.26	3.0±0.6	3.1±0.6
V	480±60	0.04	2.1±0.5	(1.1±0.2)
Cr	320±70	0.15	0.8±0.4	(0.20±0.04)
Mn	390±50	0.12	1.2±0.3	(0.8±0.2)
Fe	460±60	0.06	1.7±0.4	(3.0±0.6)
Co	640±70	0.14	3.1±0.7	(1.7±0.3)
Ni	380±40	0.13	1.1±0.2	1.1±0.2
Cu	470±50	0.09	1.8±0.4	1.5±0.3
Zn	480±50	0.13	2.4±0.5	(1.5±0.3)
Sr	210±30	0.27	1.7±0.5	
Nb	470±60	0.13	2.7±0.7	(1.3±0.3)
Mo	420±50	0.12	1.9±0.5	(0.8±0.2)
Ru	215±30	0.18	0.4±0.1	(0.4±0.1)
Rh	230±40	0.09	0.5±0.2	(1.7±0.4)
Pd	800±90	0.03	6.3±1.3	1.1±0.2
Ag	330±40	0.14	1.3±0.3	1.2±0.3
Cd	360±40	0.18	1.9±0.4	(2.5±0.5)
In	520±50	0.02	4.8±0.9	
Sn	130±20	0.08	0.3±0.1	
Sb	720±70	0.13	11±2	
Ba	490±70	0.21	9.9±2.9	
Ta	270±30	0.13	0.9±0.2	(1.1±0.2)
W	250±30	0.29	0.7±0.2	(0.8±0.2)
Re	230±30	0.14	0.5±0.1	(0.3±0.1)
Ir	200±40	0.23	0.4±0.2	(2.2±0.5)
Pt	670±50	0.06	4.6±0.7	3.9±0.8
Au	280±50	0.18	0.9±0.3	1.5±0.3
Tl	550±90	0.01	5.8±1.2	(7.4±1.5)
Pb	480±50	0.04	4.3±0.9	
Bi	540±60	0.12	6.9±1.5	

Previous Results 2

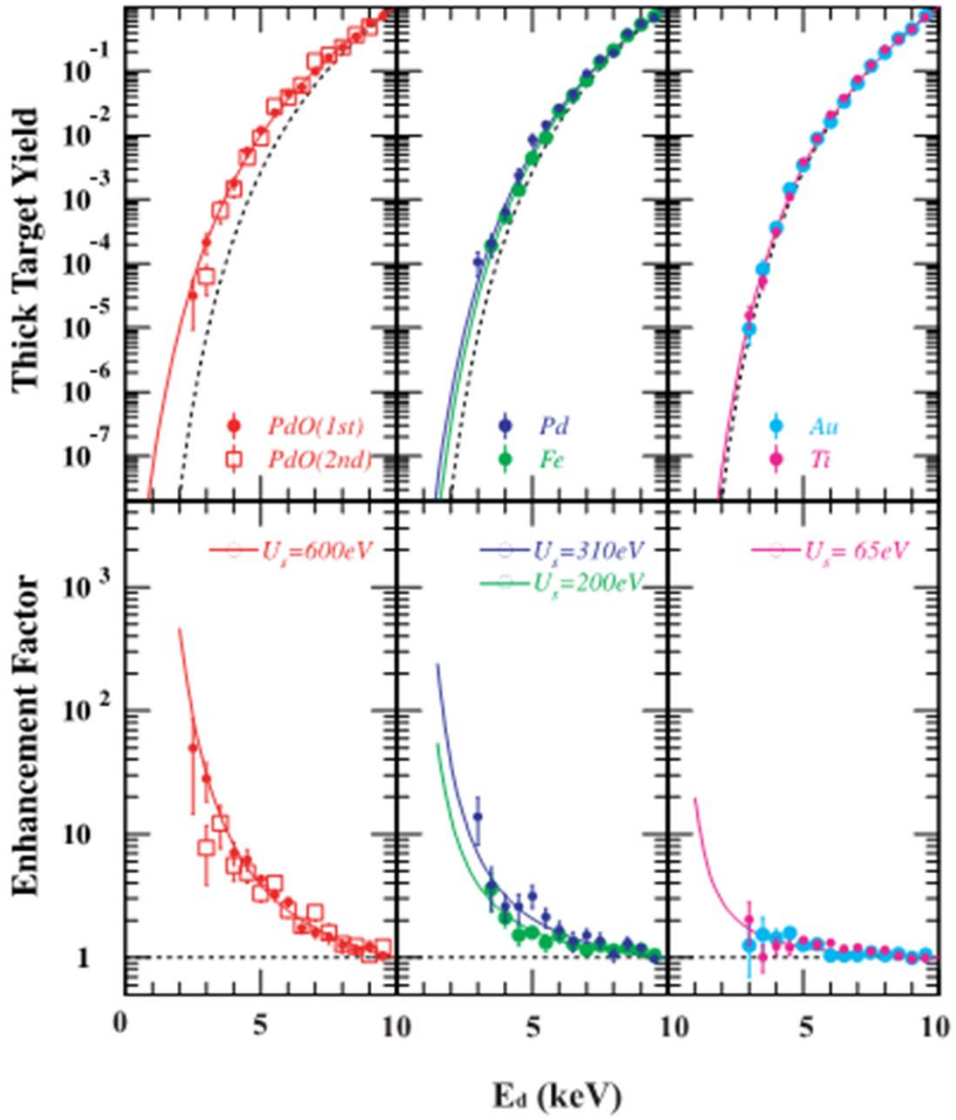

J. Kasagi, Prog. Theo. Phys. Suppl. 154 (2004) 365.

for the d(d,p)t reaction
U_e=310±30 eV @ 7% H/Pd

=> concentration dependence

Previous Results 3

for d(d,p)t reaction from K. Czerski, Phys. Rev. C **106** (2022) L011601.

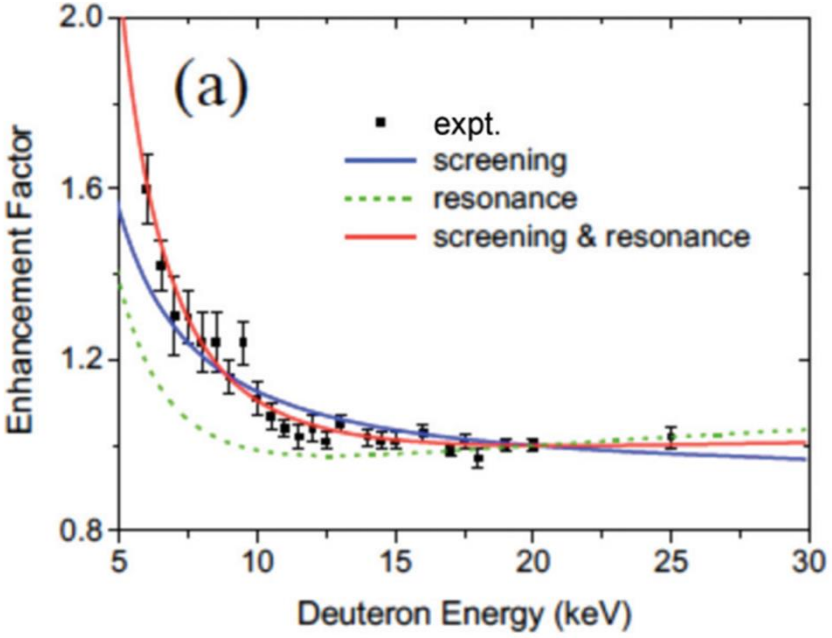

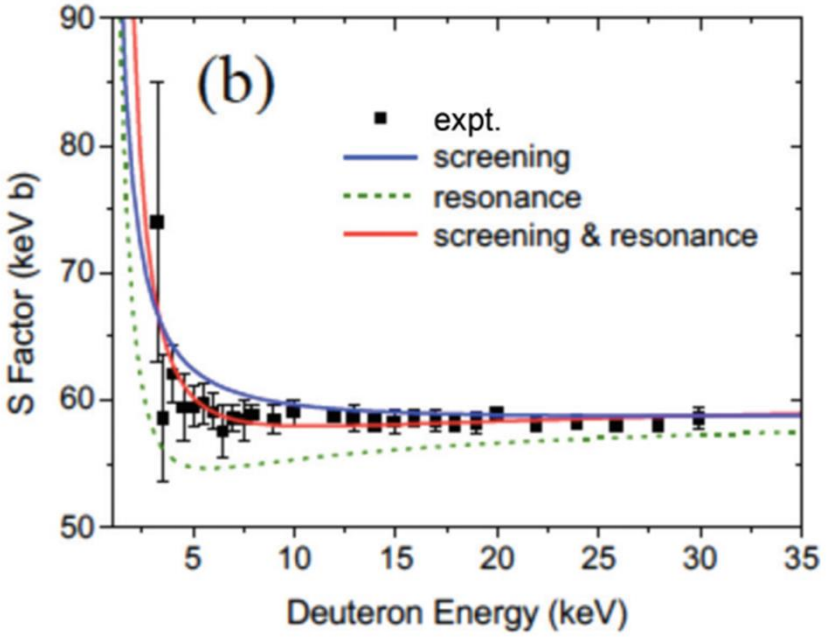

for zirconium metal
U_e=115±15 eV

for deuterium gas target
U_e≈20 eV

Previous Results 4

J. Cruz et al., Phys. Lett. B 624 (2005) 181; J. Phys. G 35 (2008) 014004.

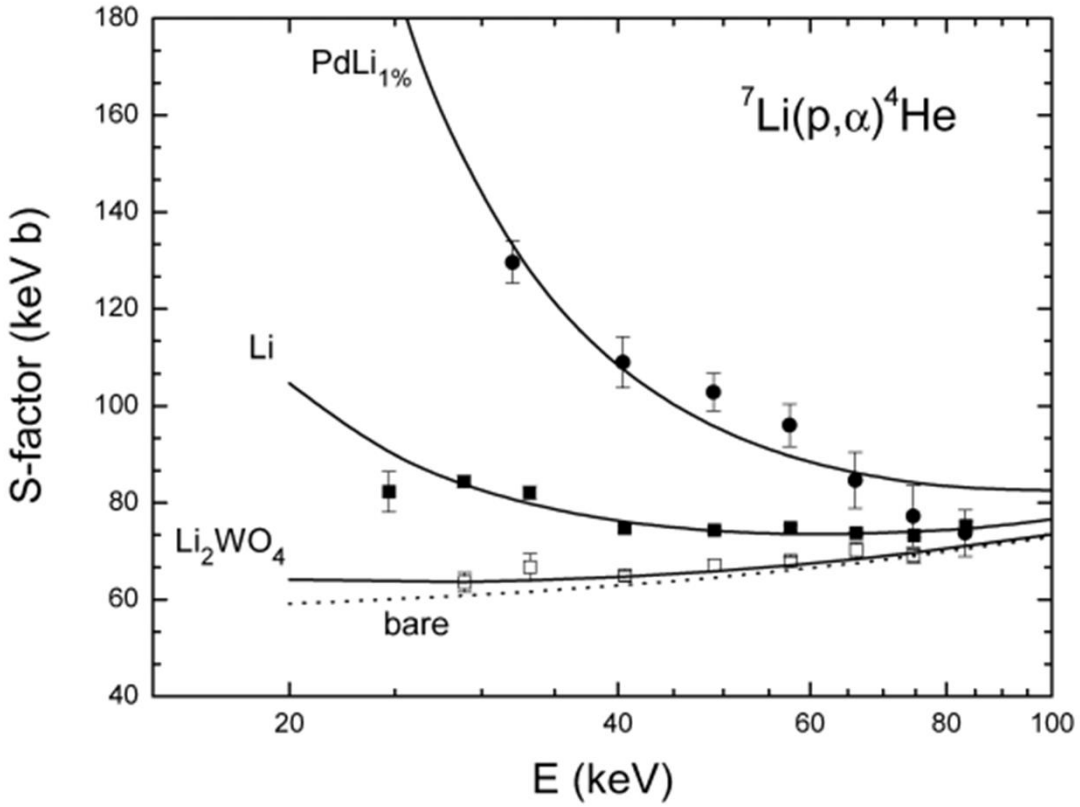

$PdLi_{1\%}$: $U_e = 3.7 \pm 0.3$ keV

Li metal: $U_e = 1.18 \pm 0.06$ keV

Li_2WO_4: $U_e = 237^{+133}_{-77}$ eV

$S(E)=0.055+0.21E-0.31E^2$[MeV b]

Previous Results 5

L. Lamia et al., Astron. Astrophys. 541, A158 (2012).

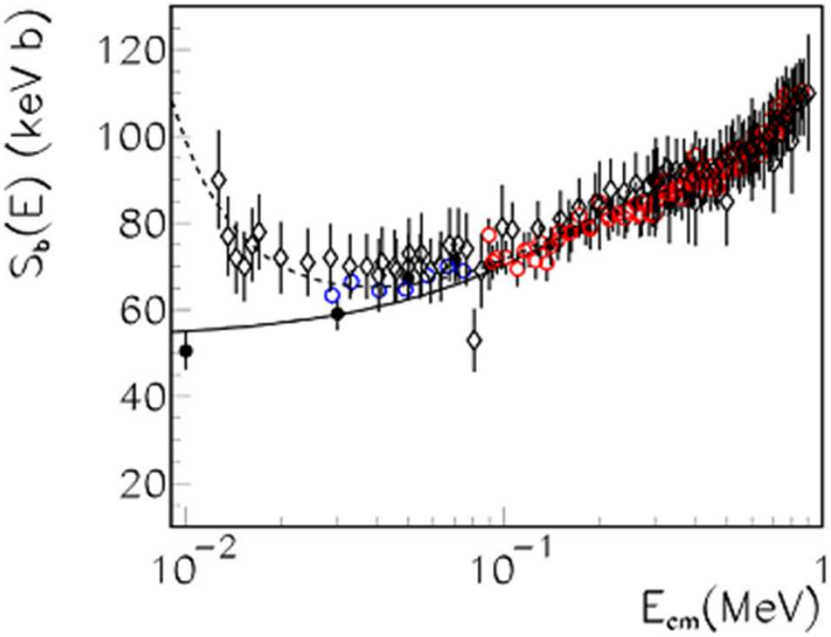

Trojan horse method → bare S factor

$S(E)=0.053+0.213E-0.336E^2$[MeV b]

^{7}Li(p,α)^{4}He reaction

$U_e = 425 \pm 60$ eV in Li metal

Adiabatic limit: $U_e = 240$ eV

Kinematics

Normal kinematics:

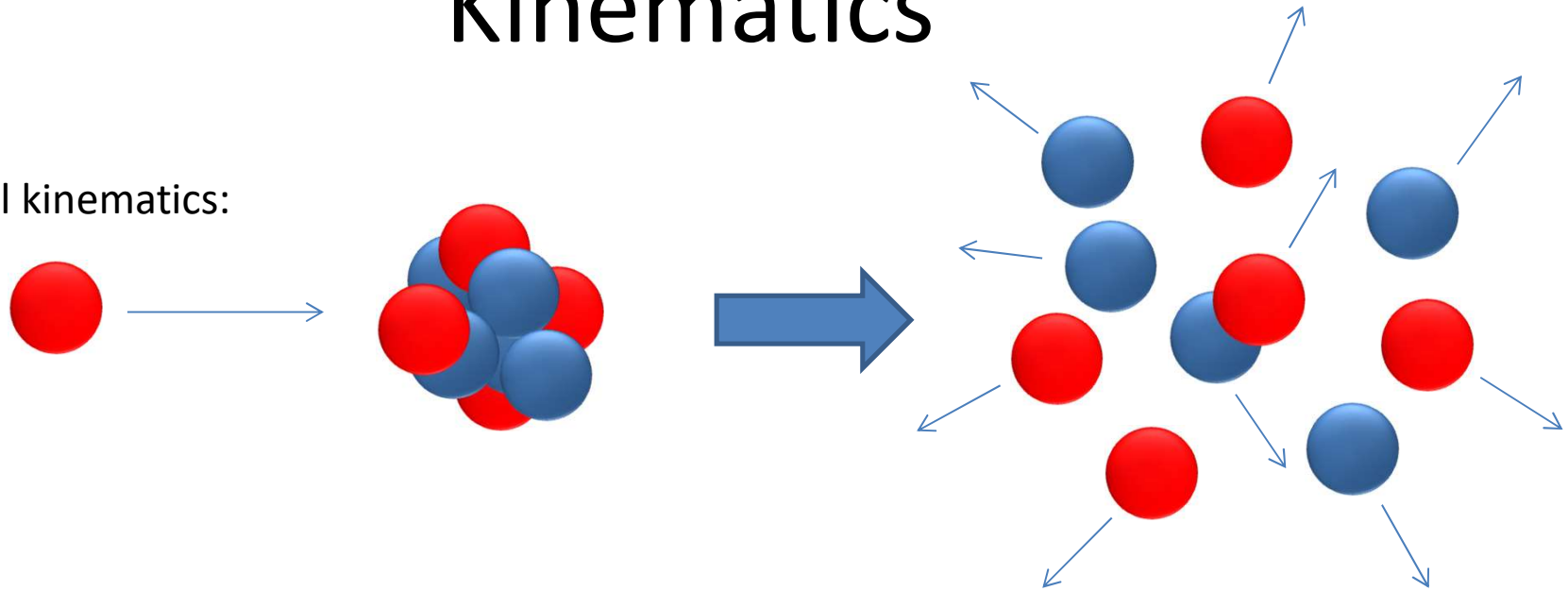

Inverse kinematics:

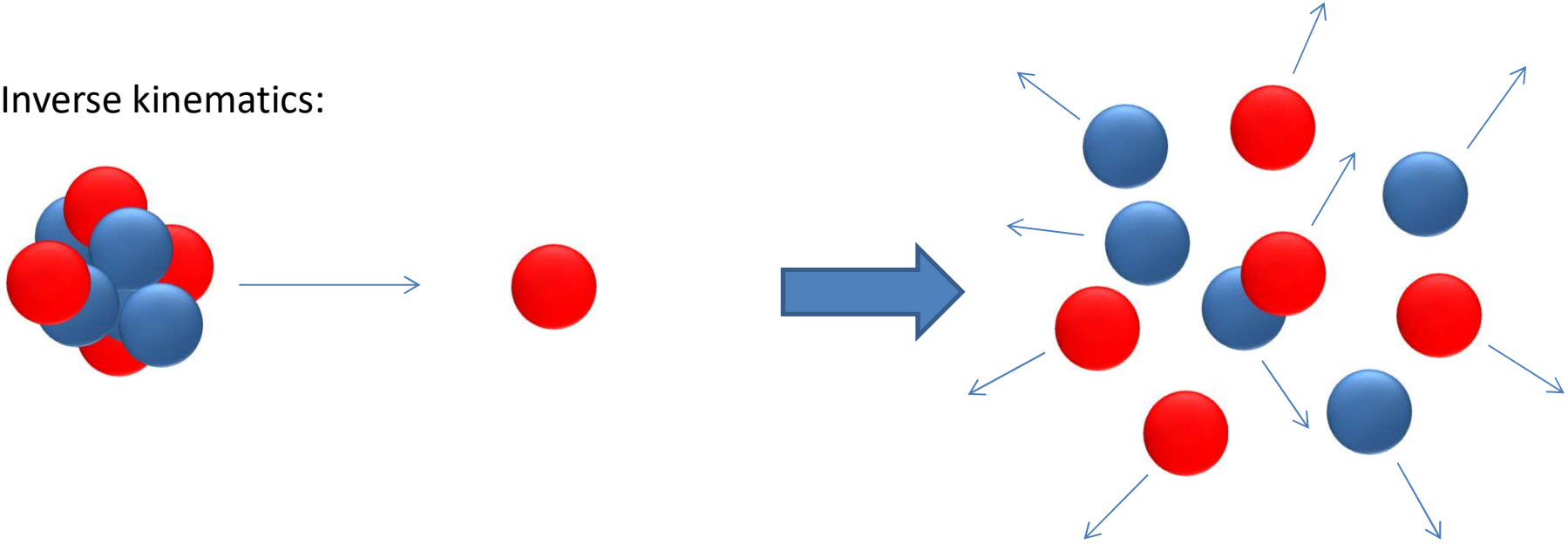

2 MV accelerator at JSI

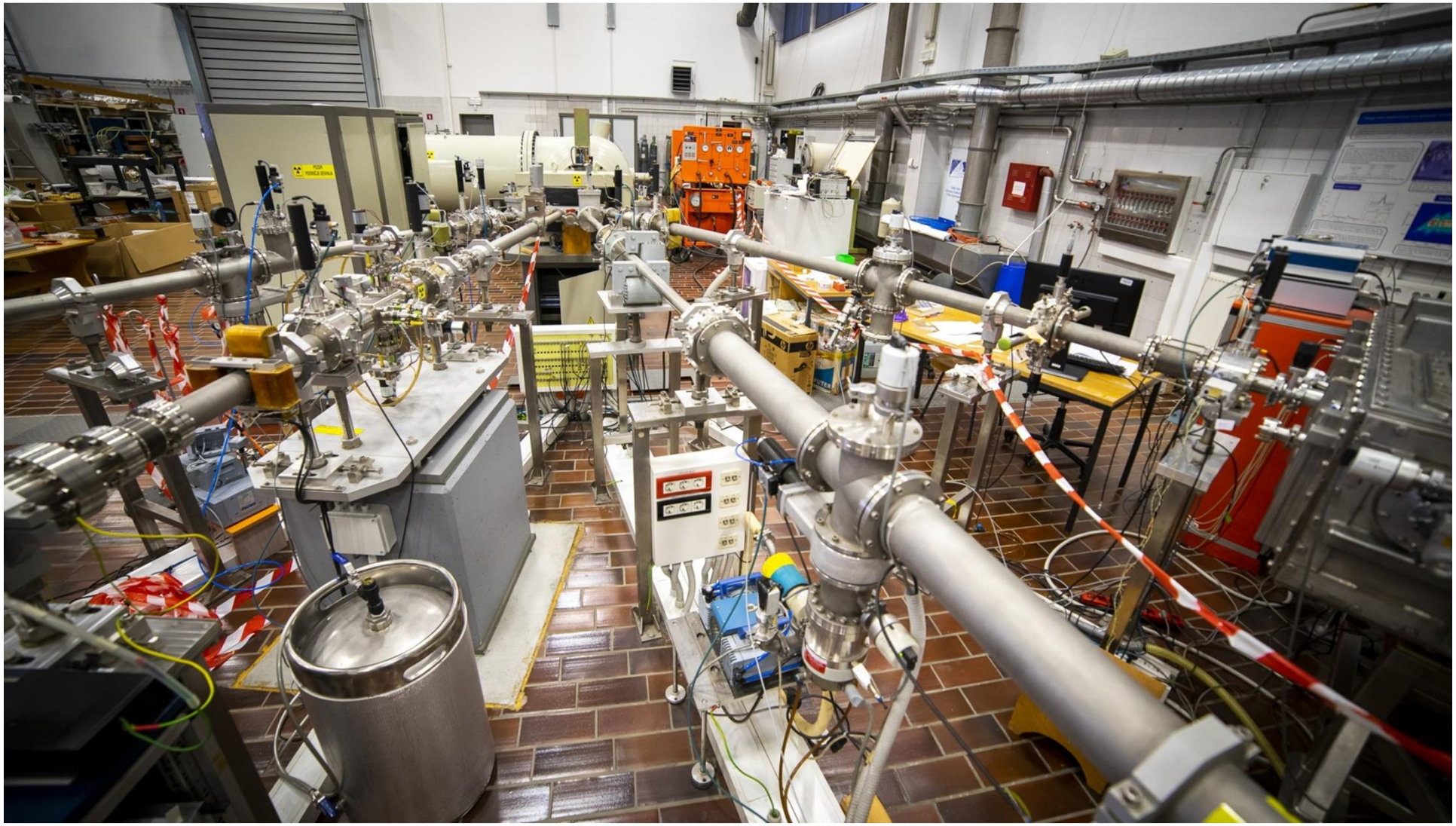

Measurements @ JSI

2 MV Tandem van de Graaf accelerator

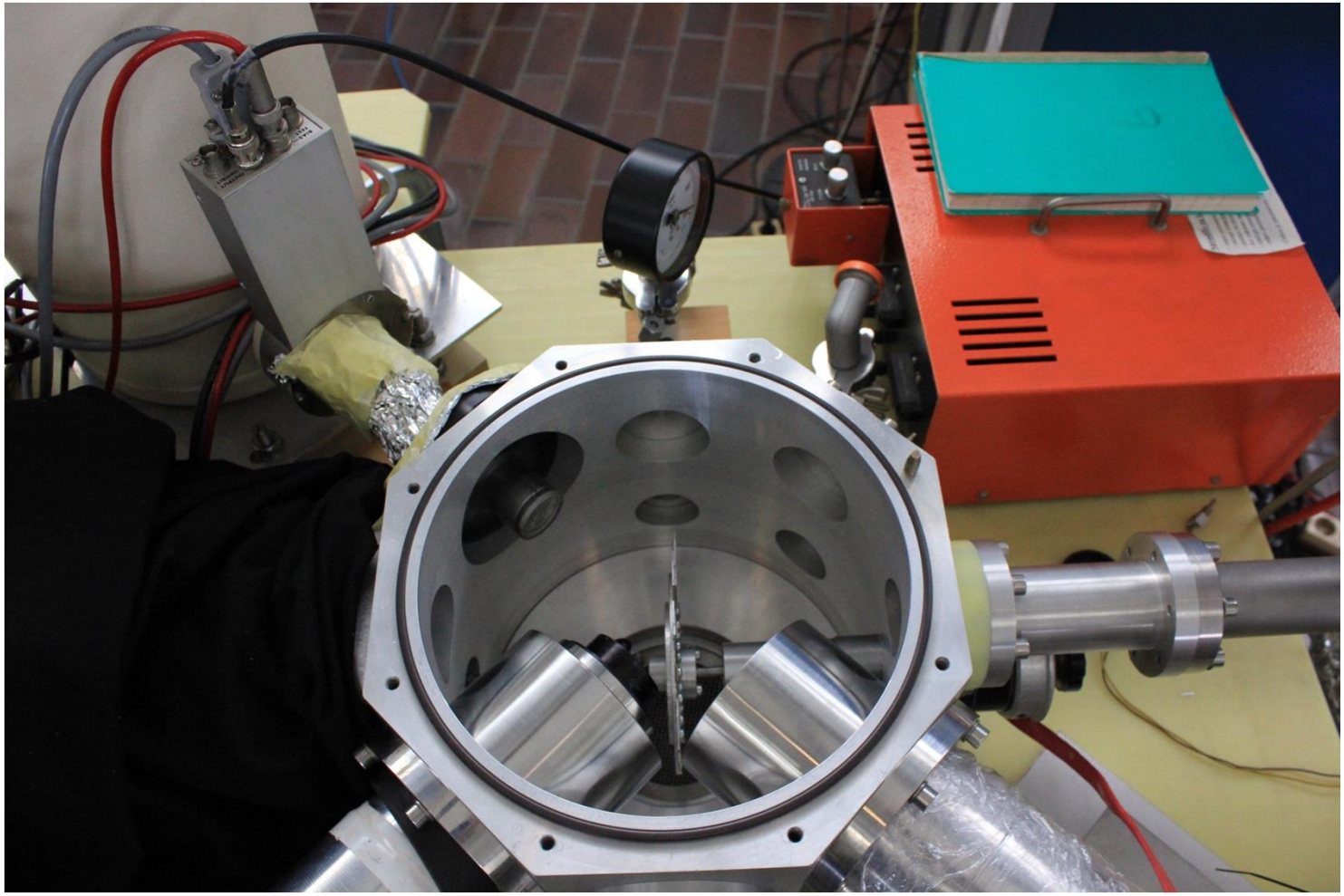

Implanted deuterium targets

Deuterium implanted into graphite or titanium at 3.5 kV resulting in up to 150 at. % deuterium concentration.

Proton beam energy between 260 and 300 keV from the 2MV Tandetron accelerator.

$^{1}H(^{2}H,\gamma)^{3}He$

^{2}H in Titanium

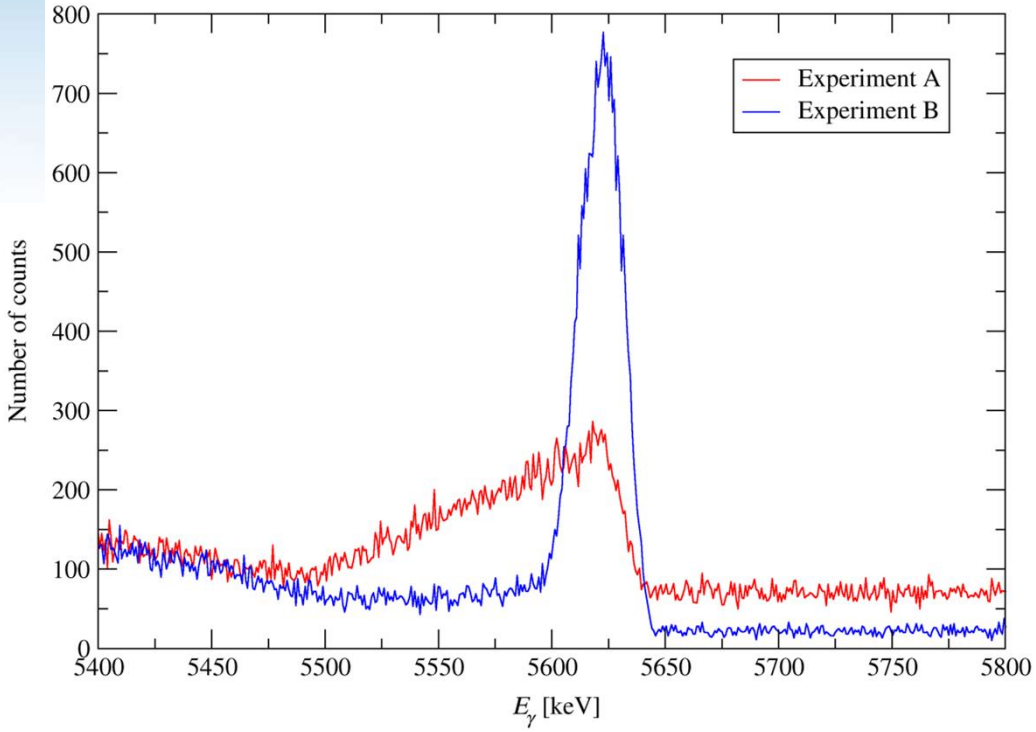

Gas loaded deuterium targets

Gas loading at room temperature, 1 atm.
Up to 70 at. % of hydrogen in Pd determined gravimetrically and checked by NRA.

Deuterium depth distribution

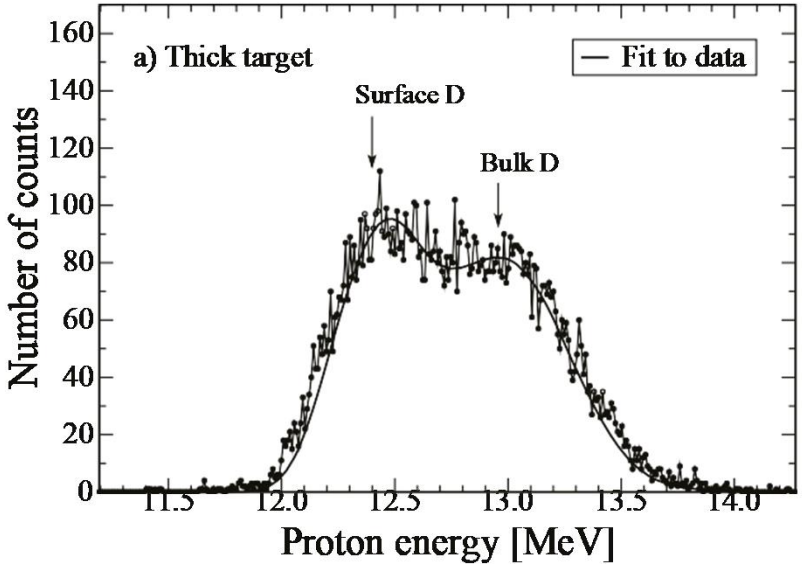

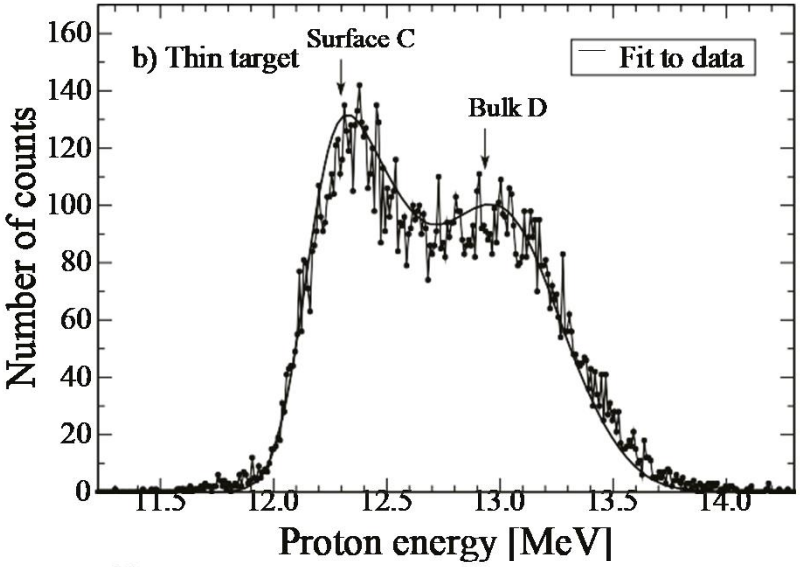

$^{2}H(^{3}He,p)^{4}He$

^{2}H in Titanium

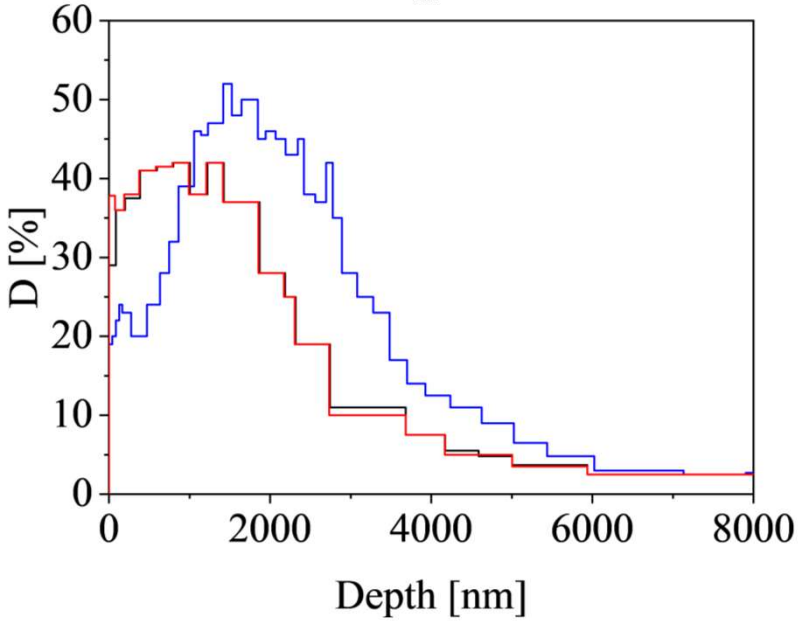

Deuterium in Palladium

$^{2}H(^{3}He,p)^{4}He$, ^{2}H in Palladium

Hard Palladium

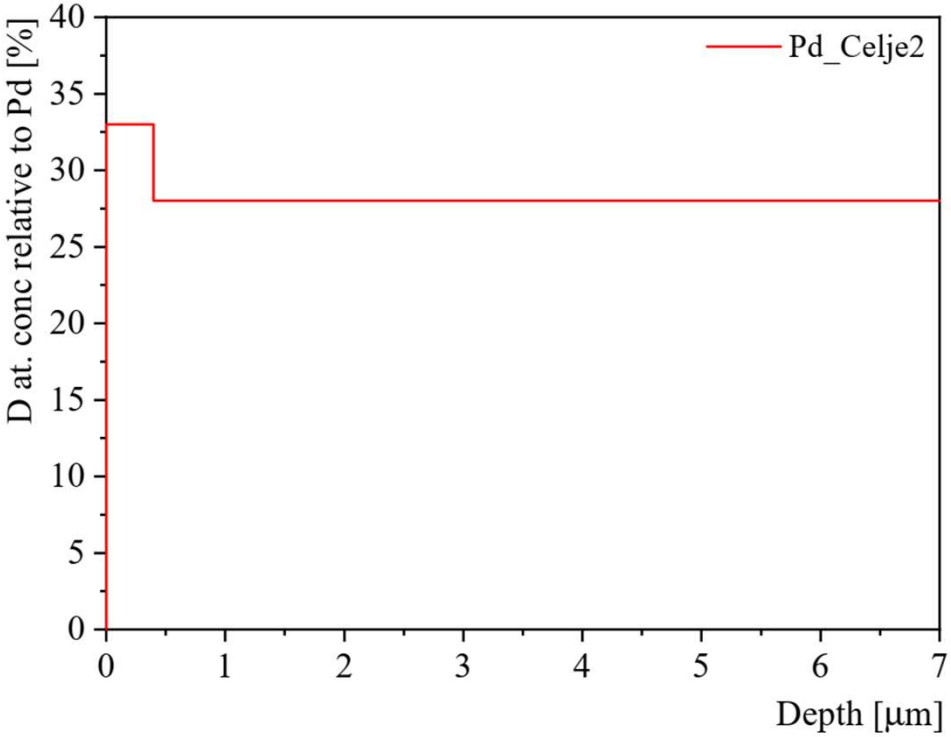

Soft Palladium

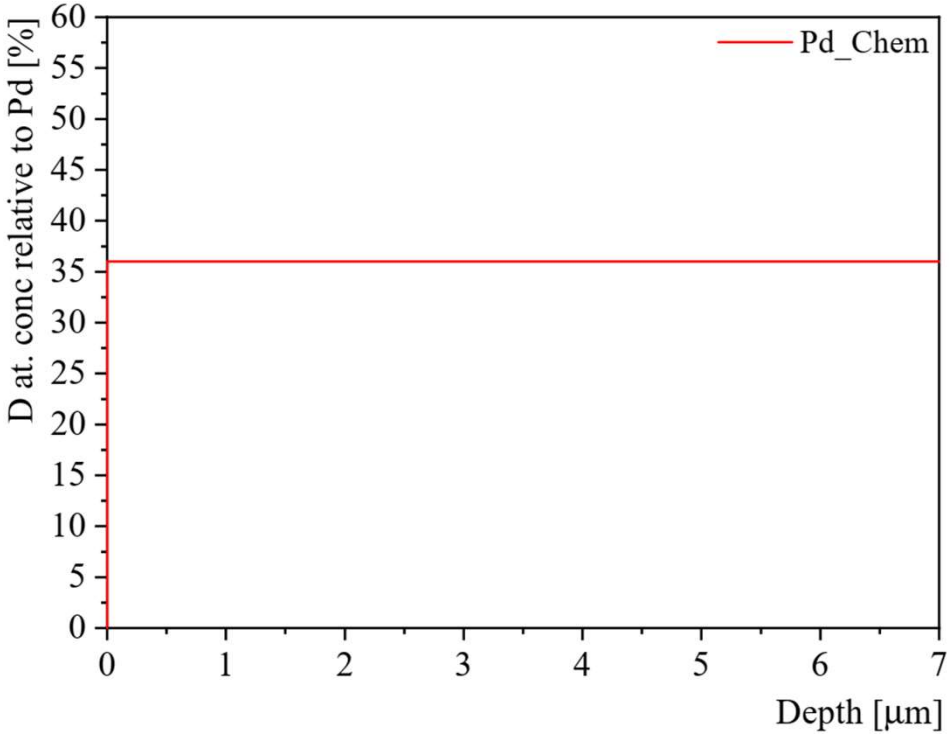

Hydrogen in Palladium

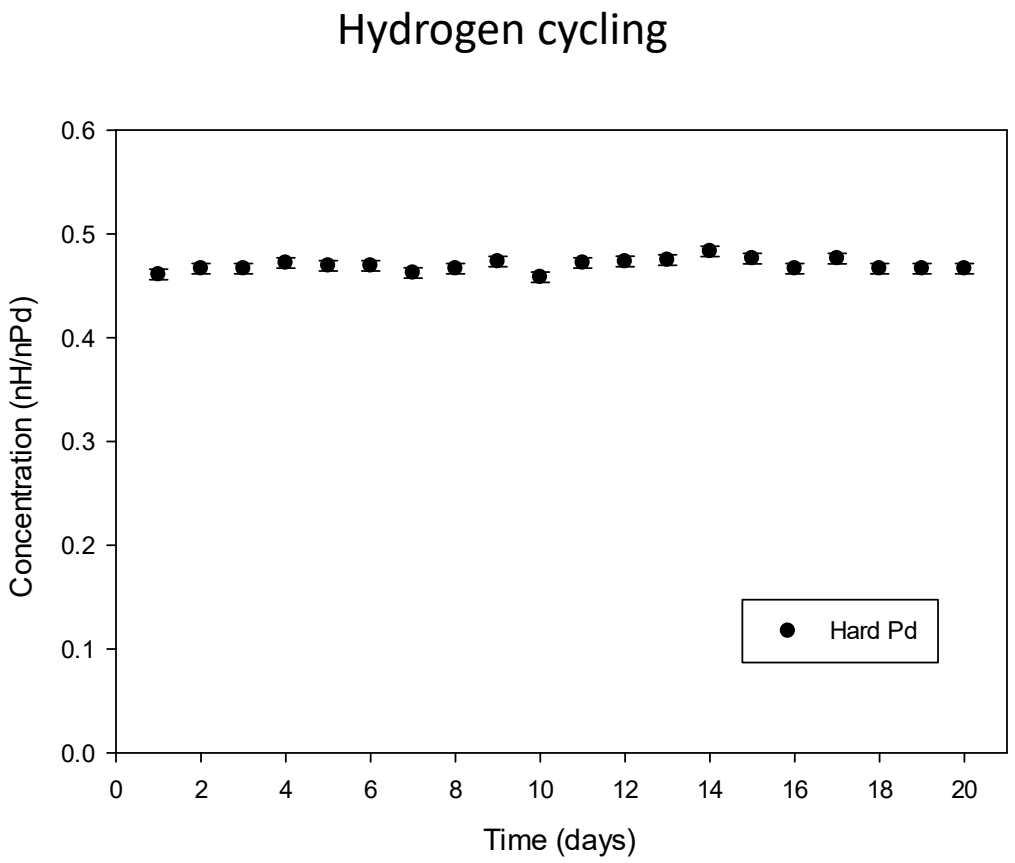

Hydrogen in Palladium

Physics Letters B 838 (2023) 137684

Contents lists available at ScienceDirect

Physics Letters B

journal homepage: www.elsevier.com/locate/physletb

Electron screening in palladium

A. Cvetinović [a,*], D. Đeorđić [b,c], G.L. Guardo [d,e], M. Kelemen [a,c], M. La Cognata [d], L. Lamia [d,e,f], S. Markelj [a], U. Mikac [a], R.G. Pizzone [d], T. Schwarz-Selinger [g], I. Tišma [a,h], M. Vencelj [a], J. Vesić [a], M. Lipoglavšek [a]

[a] *Jožef Stefan Institute, Ljubljana, Slovenia*
[b] *University of Banja Luka, Faculty of Mechanical Engineering, Banja Luka, Bosnia and Herzegovina*
[c] *Jožef Stefan International Postgraduate School, Ljubljana, Slovenia*
[d] *INFN-Laboratori Nazionali del Sud, Catania, Italy*
[e] *Dipartimento di Fisica e Astronomia "E. Majorana", University of Catania, Catania, Italy*
[f] *Centro di Fisica Nucleare e Struttura della Materia, University of Catania, Catania, Italy*
[g] *Max Planck Institute for Plasma Physics, Garching, Germany*
[h] *Ruđer Bošković Institute, Zagreb, Croatia*

Fluorine + Deuterium

Normal kinematics:

$^{19}F(^{2}H,p)^{20}F$

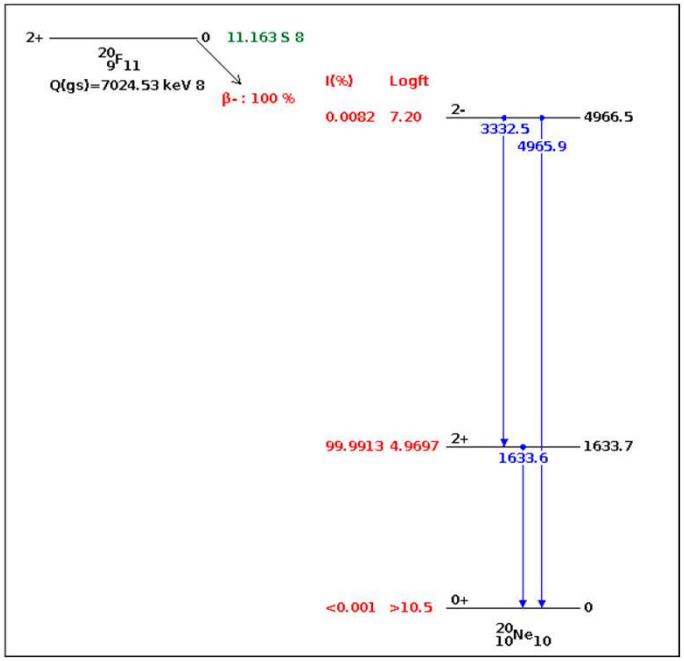

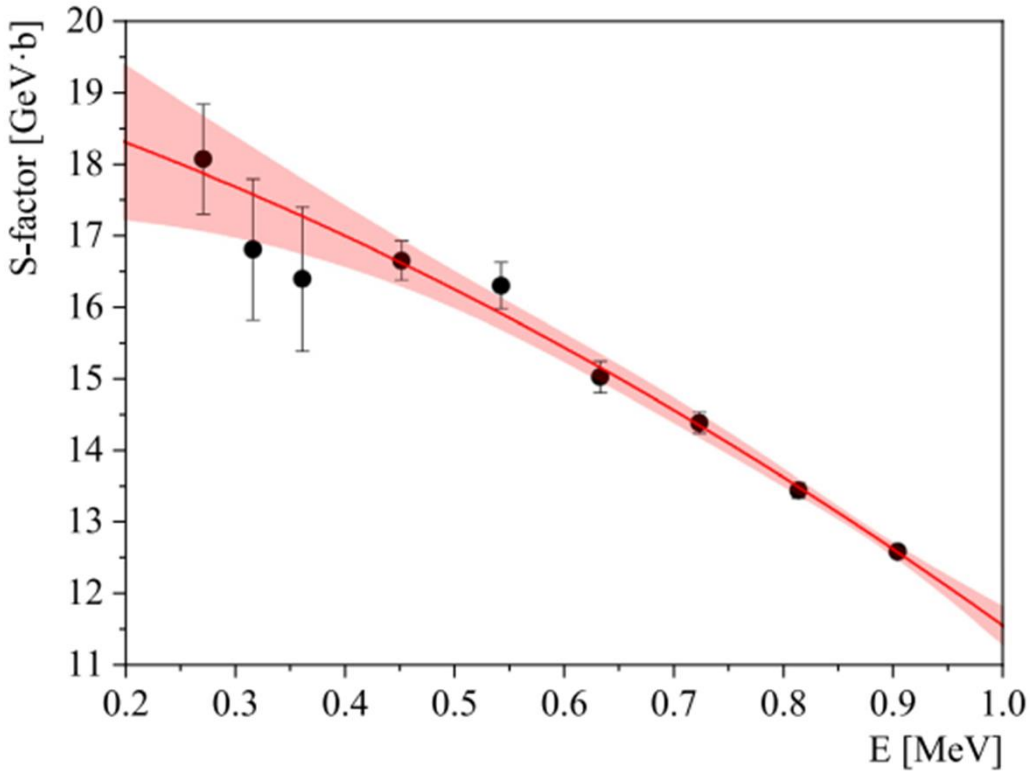

$^{2}H(^{19}F,p)^{20}F$

$^{20}F \rightarrow {}^{20}Ne + e^{-} + \nu + \gamma$ $\quad E_{\gamma}=1634$ keV

CaF_2 target; JSI + MPI Garching

Deuterium in Palladium

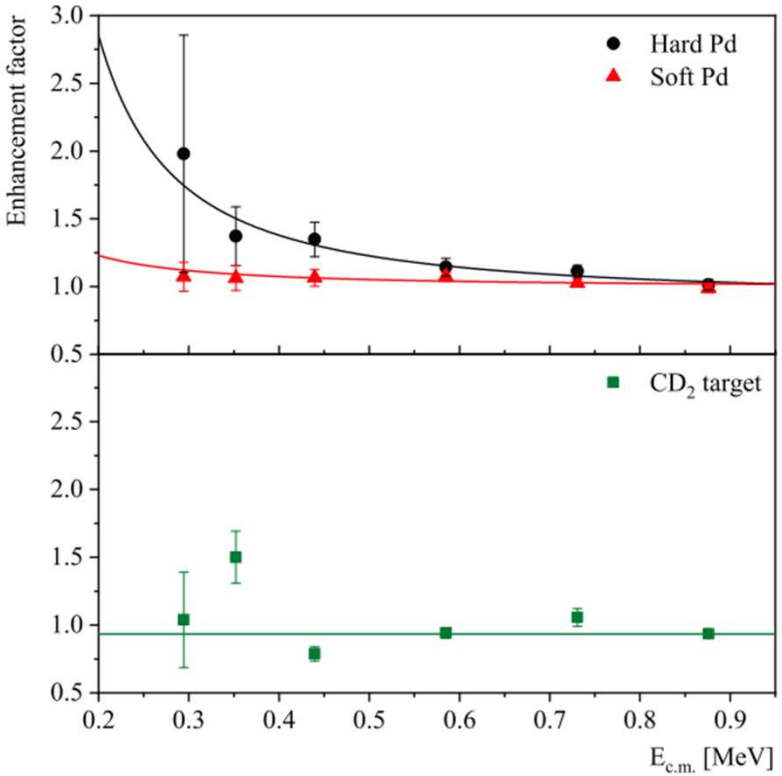

Hard Pd: $U_e = 18.2 \pm 3.3$ keV

Soft Pd: $U_e = 3.2 \pm 1.9$ keV

Adiabatic limit:
$U_e = 2.19$ keV

CD_2: $U_e < 3.0$ keV

Fluorine + Protons

$^{1}H(^{19}F,\alpha\gamma)^{16}O$

Enhancement factor:

$$f = \frac{e^{-2\pi\eta(E+Ue)}}{e^{-2\pi\eta(E)}} = \frac{\omega\gamma_1}{\omega\gamma_2}$$

$$f = 1.53 \rightarrow$$

$$U_e = 18.7 \pm 1.5\ keV$$

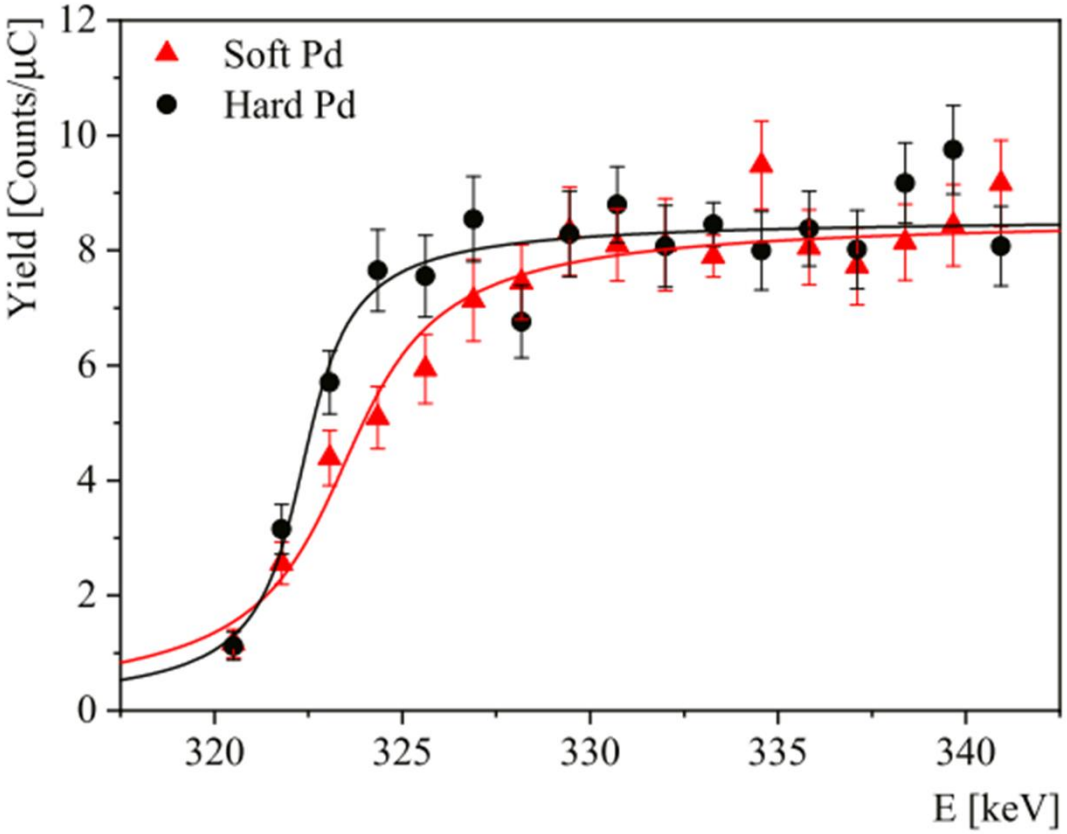

^{7}Li + Protons

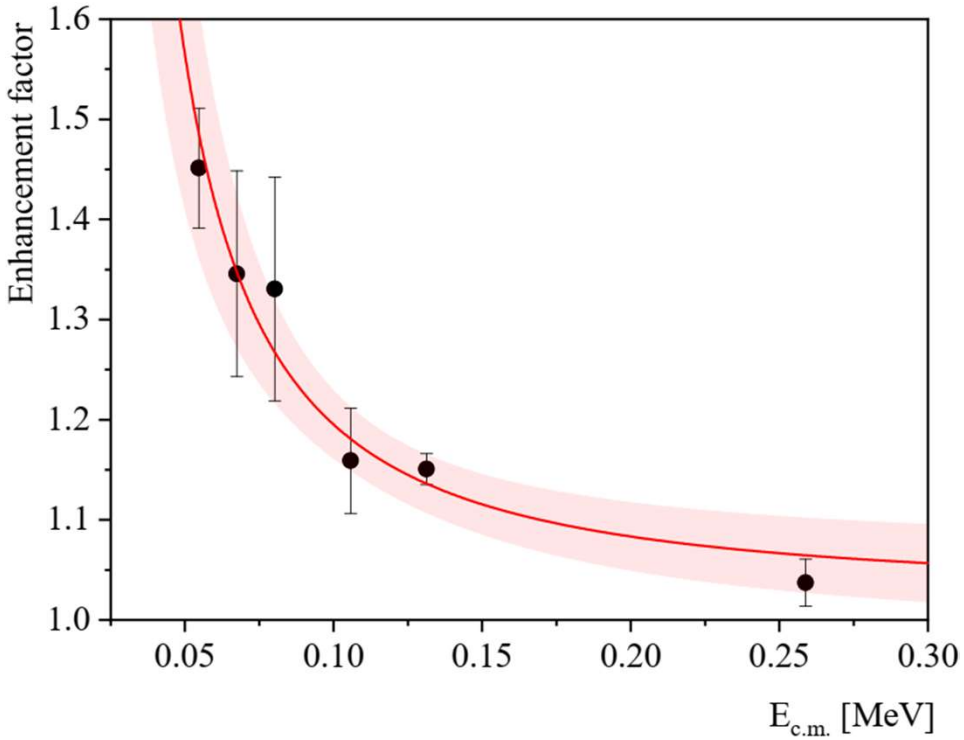

^{1}H(^{7}Li,α)^{4}He

Hard Pd: U_e=2.86 ± 0.19 keV
Adiabatic limit:
U_e= 0.24 keV

$U_e = U_0 Z^2$ $U_0 \approx$ 300 eV

^{6}Li + Deuterium

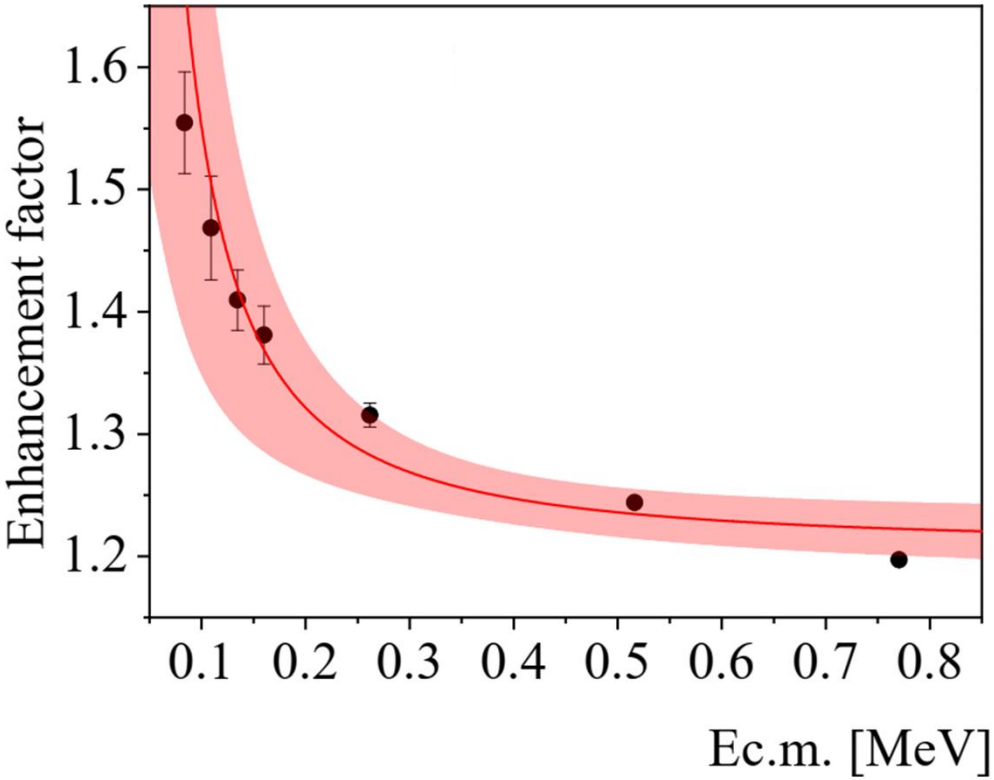

^{2}H(^{6}Li,α)^{4}He

Hard Pd: U_e=4.48 ± 0.10 keV
Adiabatic limit:
U_e= 0.24 keV

Isotope effect???

NMR Spectroscopy

Knight's shift K_H:

$$K_H = S(0^\circ) - \frac{4\pi}{3}\chi_v - \sigma.$$

Knight's shift is proportional to the density of electrons at the place of the proton

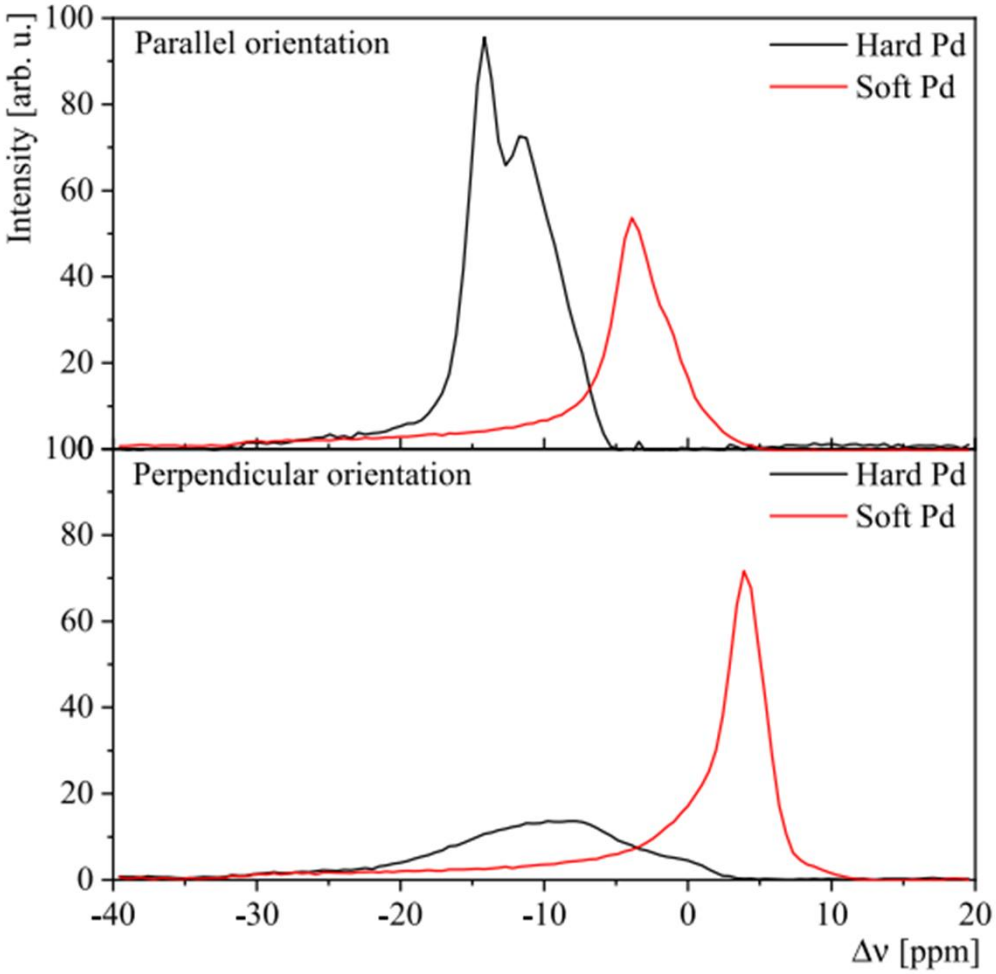

Conclusions

- Electron screening depends on the position of hydrogen nuclei in the crystal lattice.
- Electron screening is not proportional to Z, more likely Z^2.
- Lithium seems to have disproportionally large electron
- Link between metals and plasma is an unfulfilled wish.

Crystal symmetry

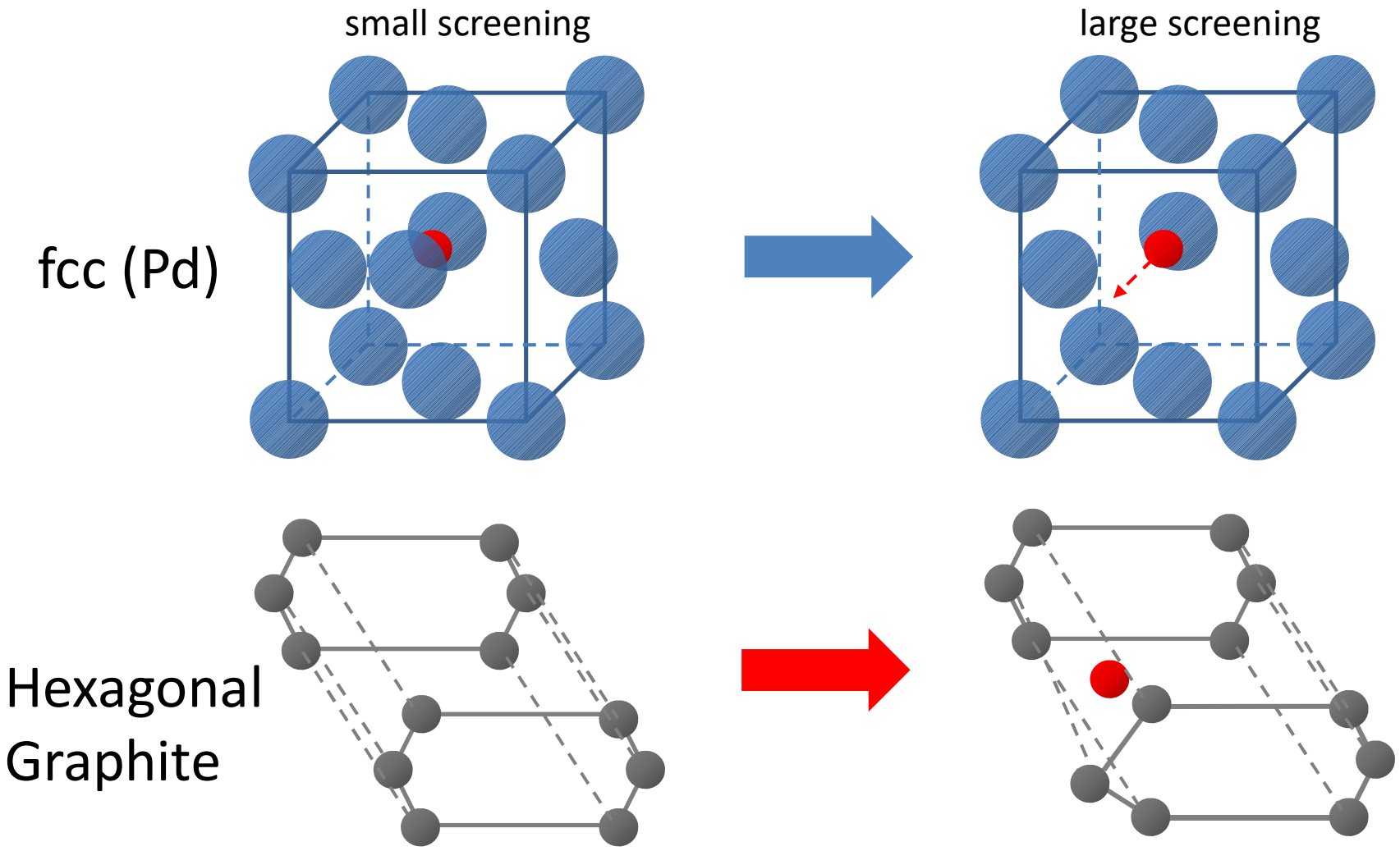

Electrons

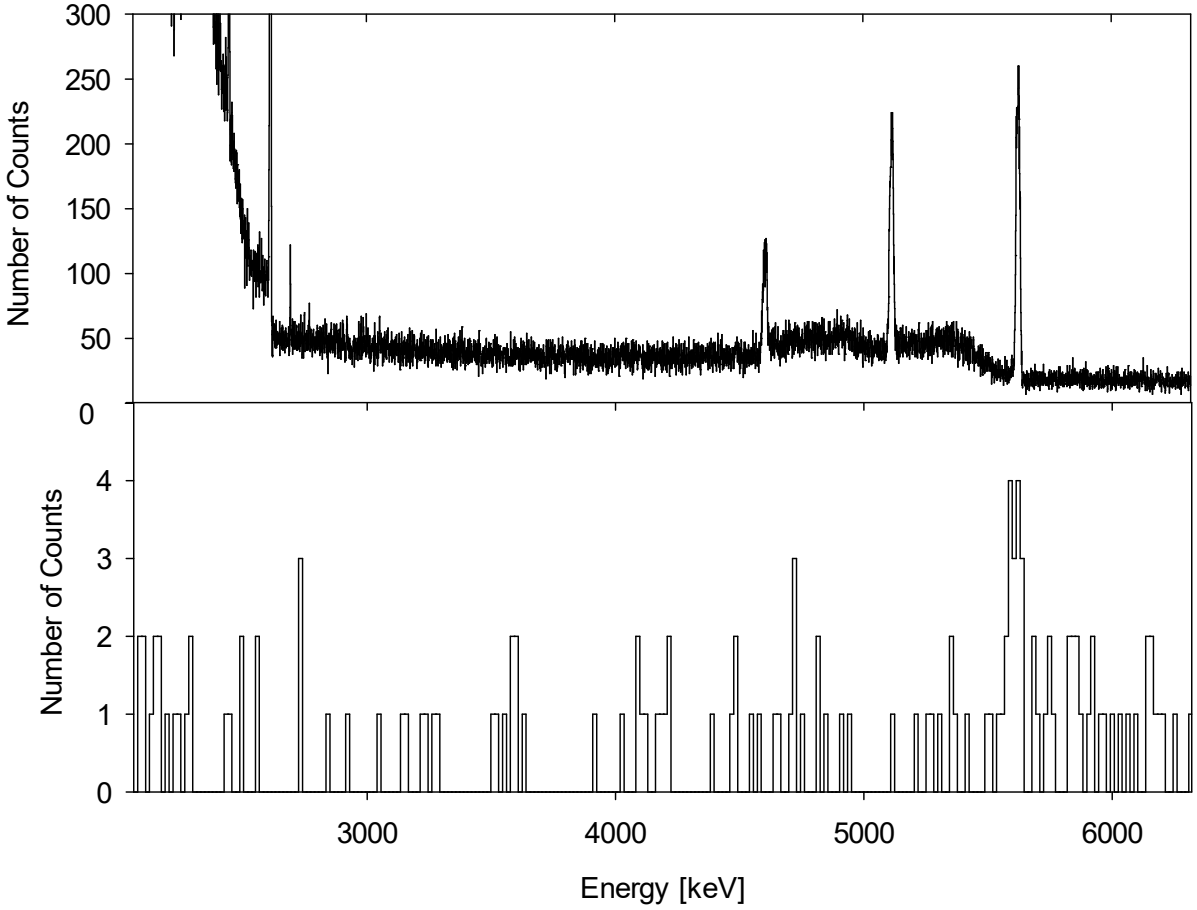

$^{2}H(p,\gamma)^{3}He$

$^{2}H(p,e^{-})^{3}He$

Bi-207 source

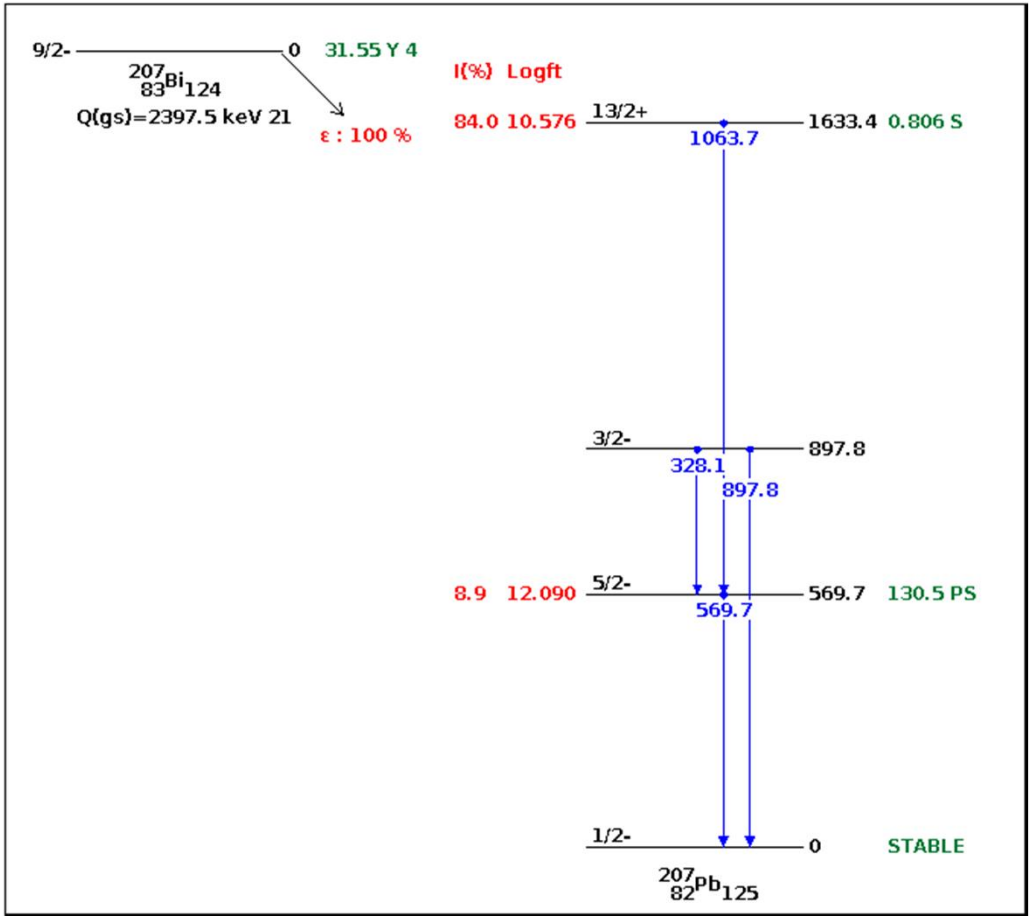

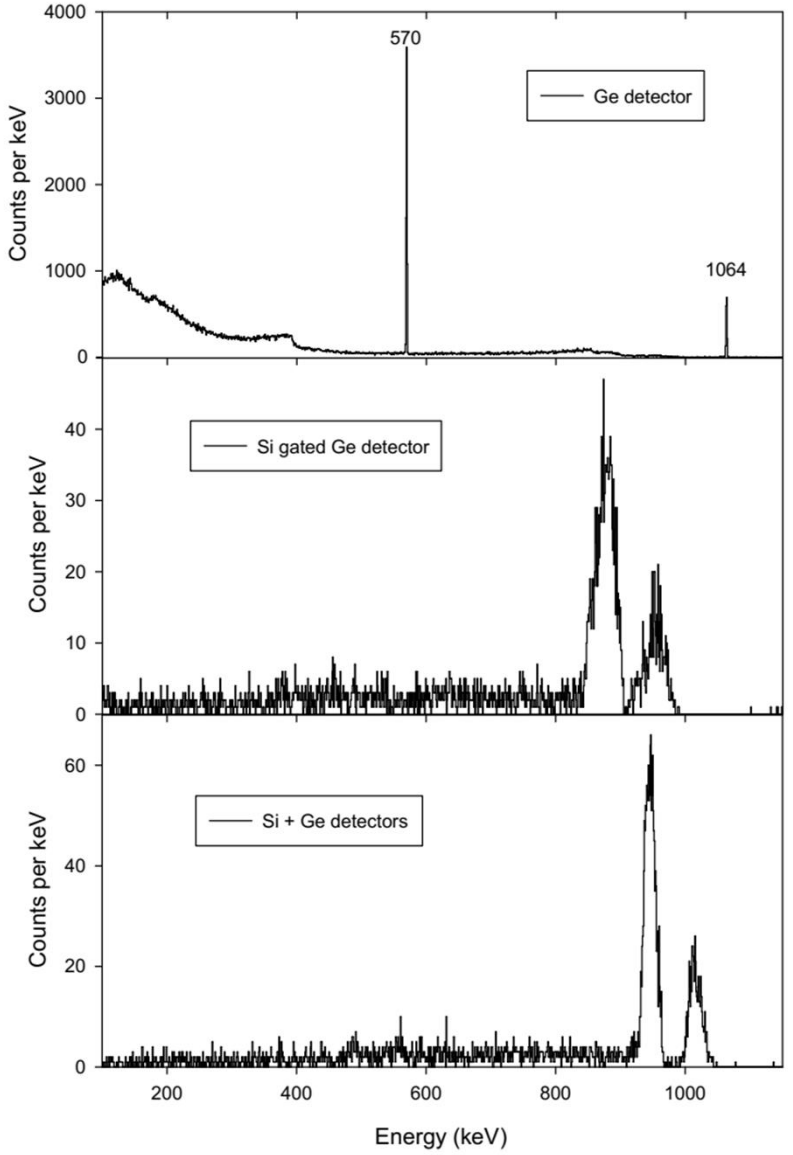

The $^{19}F(p,\alpha\gamma)^{16}O$ Reaction

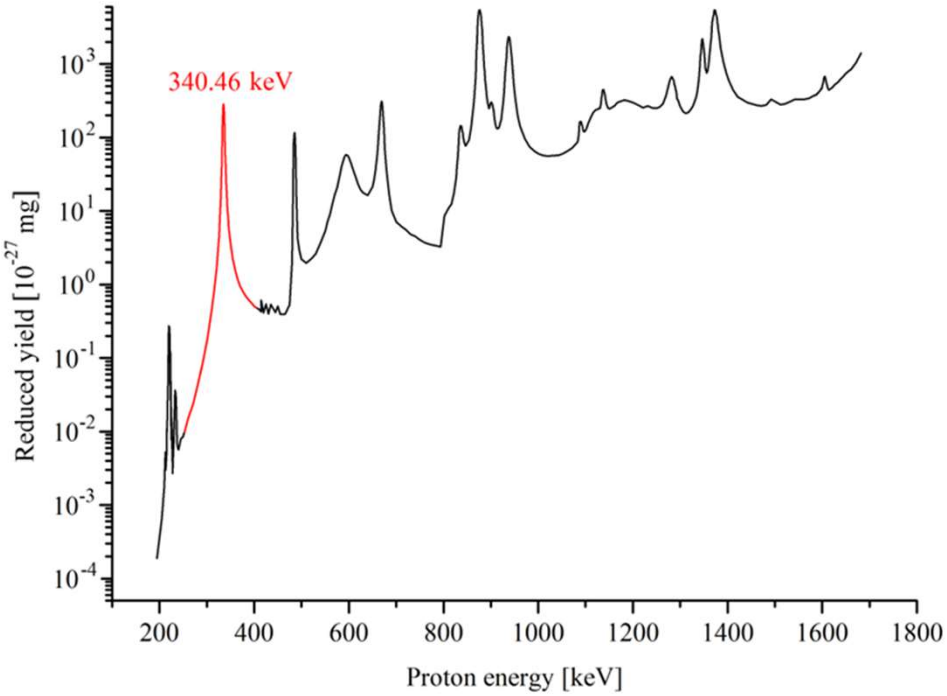

K. Spyrou et al., Z. Phys. A **357** (1997) 283;
Eur. Phys. J. A **7** (2000) 79.

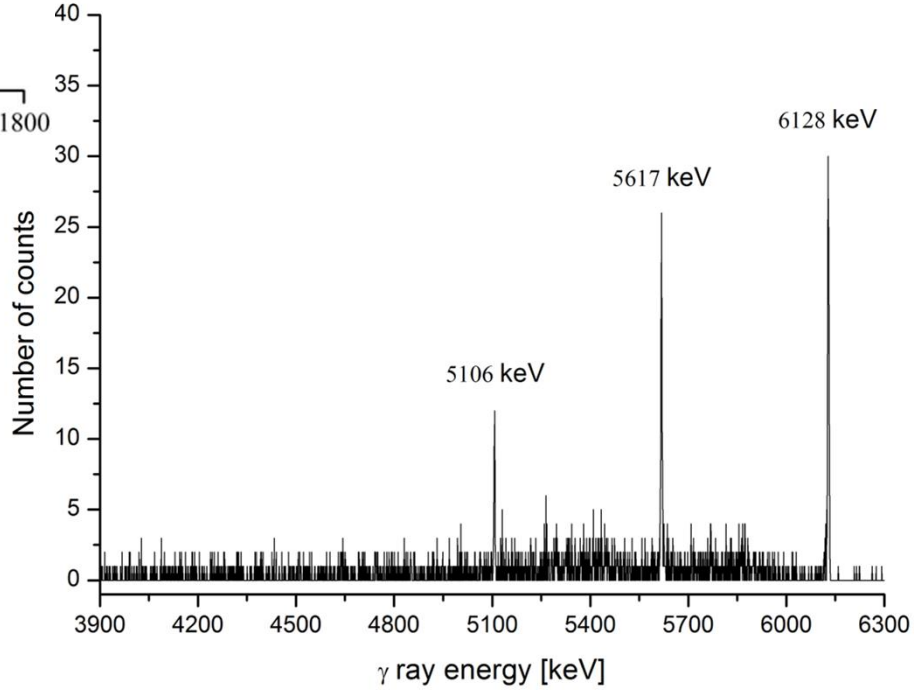

Thick targets and resonances

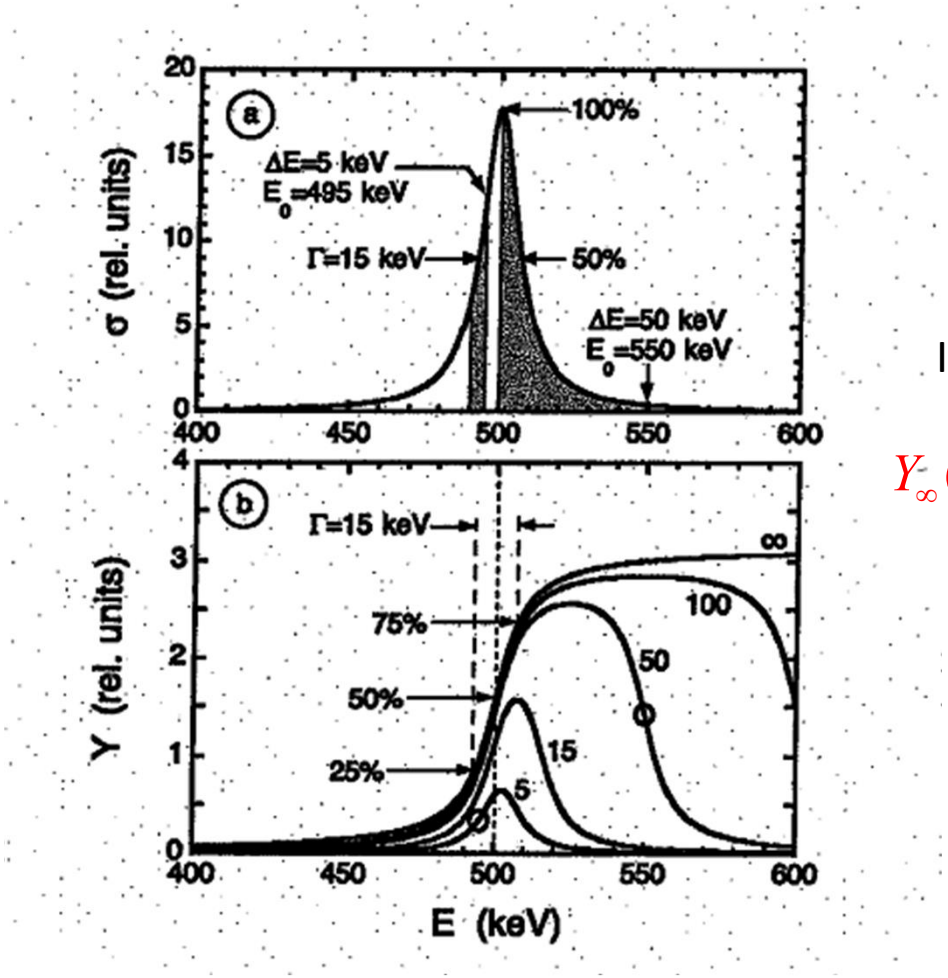

Breit Wigner resonance cross section

$$\sigma(E) = \frac{\lambda^2 \omega}{4\pi} \frac{\Gamma^2}{(E_r - E)^2 + \Gamma^2},$$

Infinitely thick target yield of narrow resonance

$$Y_\infty(E) = n_X \frac{\lambda^2 \omega \gamma}{2\pi \cdot dE/dx\rho} \left[arctg\left(\frac{E - E_r}{\Gamma/2} \right) + \frac{\pi}{2} \right],$$

Integral over the resonance

$$A_Y = n \frac{\lambda^2 \omega \gamma}{2}.$$

C. Iliadis, Nuclear Physics of Stars, Wiley-VCH, Weinheim, (2007) p. 341.

Catalysis of nuclear reactions by muons

Rubin, U. S. Geological Survey Radiocarbon Laboratory, kindly communicated to the writer. (See references 9 and 10.)

[9] H. Craig, Tellus (to be published).

[10] H. Craig, reference 5.

[11] Benton, Estoque, and Dominitz, Science Report No. 1, Civil Engineering Department, Johns Hopkins University, 1953 (unpublished).

[12] W. F. Libby, Science 123, 656 (1956); Proc. Nat. Acad. Sci. 42, 365 (1956).

[13] P. Morrison and J. Pine, Ann. N. Y. Acad. Sci. 62, 69 (1955).

[14] K. Mayne, Geochim. et Cosmochim. Acta 9, 174 (1956).

[15] Fowler, Burbidge, and Burbidge, Astrophys. J. Suppl. 2, 167 (1955).

[16] M. Koshiba and M. Schein, Phys. Rev. 103, 1820 (1956).

[17] *Note added in proof.*—The results of these calculations were discussed with F. Begemann and W. F. Libby during the summer of 1956; they now find that their recent data on the tritium balance in the Mississippi Valley, taking into account outward vapor transport of tritium as discussed above, indicate a production rate over that area equal to the value calculated above for North America. Recently J. Arnold has also concluded from consideration of the present calculations that tritium is probably being accreted from the sun.

Catalysis of Nuclear Reactions by μ Mesons*

L. W. Alvarez, H. Bradner, F. S. Crawford, Jr., J. A. Crawford,† P. Falk-Vairant, M. L. Good, J. D. Gow, A. H. Rosenfeld, F. Solmitz, M. L. Stevenson, H. K. Ticho, and R. D. Tripp

Radiation Laboratory, University of California, Berkeley, California

(Received December 17, 1956)

IN the course of a recent experiment involving the stopping of negative K mesons in a 10-inch liquid hydrogen bubble chamber,[1] an interesting new reaction was observed to take place. The chamber is traversed by many more negative μ mesons than K mesons, so that in the last 75 000 photographs, approximately 2500 μ^- decays at rest have been observed. In the same pictures,

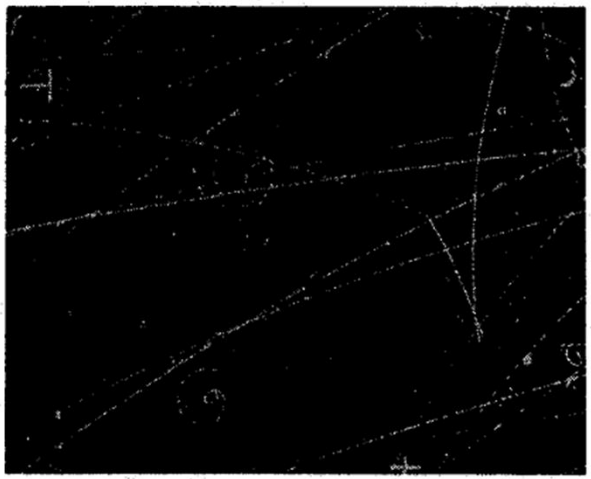

FIG. 1. Example of H-D reaction catalyzed by μ^- meson. The incident meson comes to rest, drifts as a neutral mesonic atom, is ejected with 5.4 Mev by the H-D reaction, comes to rest again after 1.7 cm, and decays.

between the last bubble of the primary track and the first bubble of the secondary track. This gap is a real effect, and not merely a statistical fluctuation in the spacing of the bubbles, since in some cases the tracks form a letter X (see Fig. 1), and in another case the secondary track is parallel to the primary, but displaced transversely by about 1 mm at the end of the primary. These real gaps appear also (although perhaps less frequently) between some otherwise normal-looking μ^- endings and the subsequent decay electron; they are thought to be the distance traveled by the small neutral mesonic atom.[3]

One may quickly dispose of the most obvious suggestion that the events are $\pi^- - \mu^- - e^-$ decays. If, by some unknown process, negative π mesons could decay

Instead of
$D(p,\gamma)^3He$
Alvarez measured
$D(p,\mu)^3He$

Clean HME Horizon 2020 Project

Clean Hydrogen Metal Energy

Project overview

CleanHME shall develop a new, clean, safe, compact and very efficient energy source based on Hydrogen-Metal and plasma systems, which could be a breakthrough for both private use as well as for industrial applications. The new energy source could be employed both as a small mobile system or alternatively as a stand-alone heat and electricity generator. We plan to construct a new compact reactor to test the HME technology during the long-term experiments and increase its technology readiness level. A comprehensive theory of HME phenomena shall be worked out as well. This project has received funding from the European Union's Horizon2020 Framework Programme under grant agreement no 951974.

https://www.cleanhme.eu/

Nuclear Fusion

$$p + D \rightarrow {}^{3}He + \gamma + 5.5\ MeV$$

$$D + D \rightarrow {}^{4}He + \gamma + 24\ MeV$$
$$\rightarrow {}^{3}He + n + 3.3\ MeV$$
$$\rightarrow T + p + 4.0\ MeV$$

$$D + T \rightarrow {}^{4}He + n + 18\ MeV$$

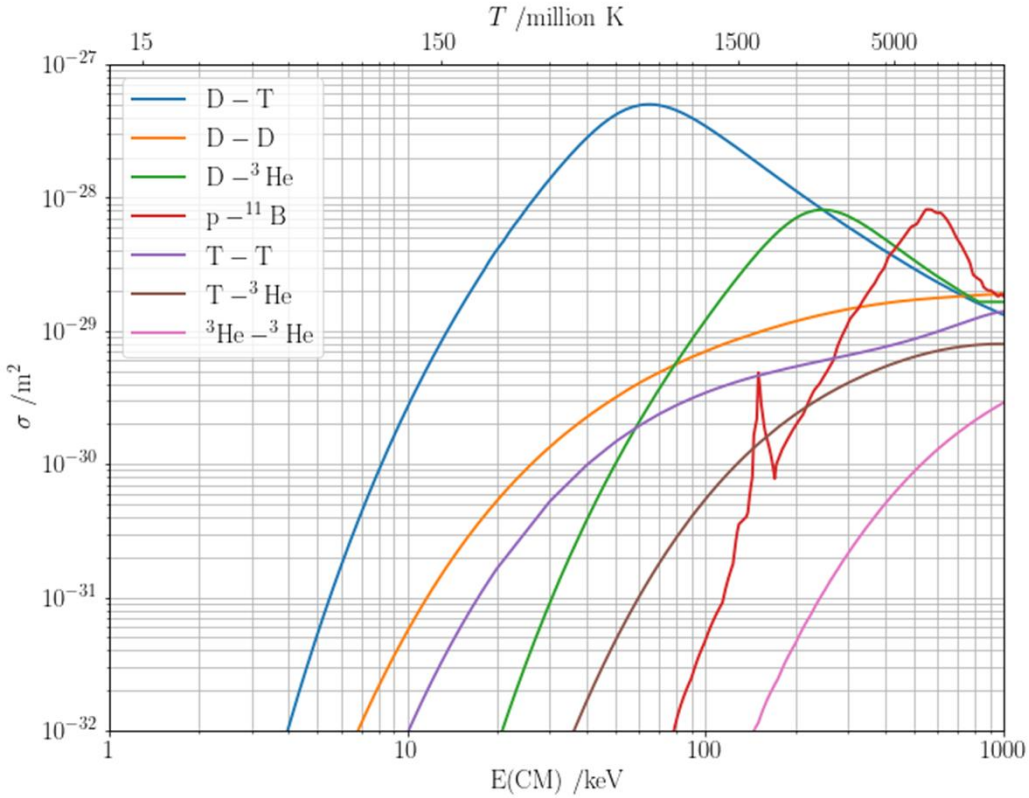

Astrophysical S-factor

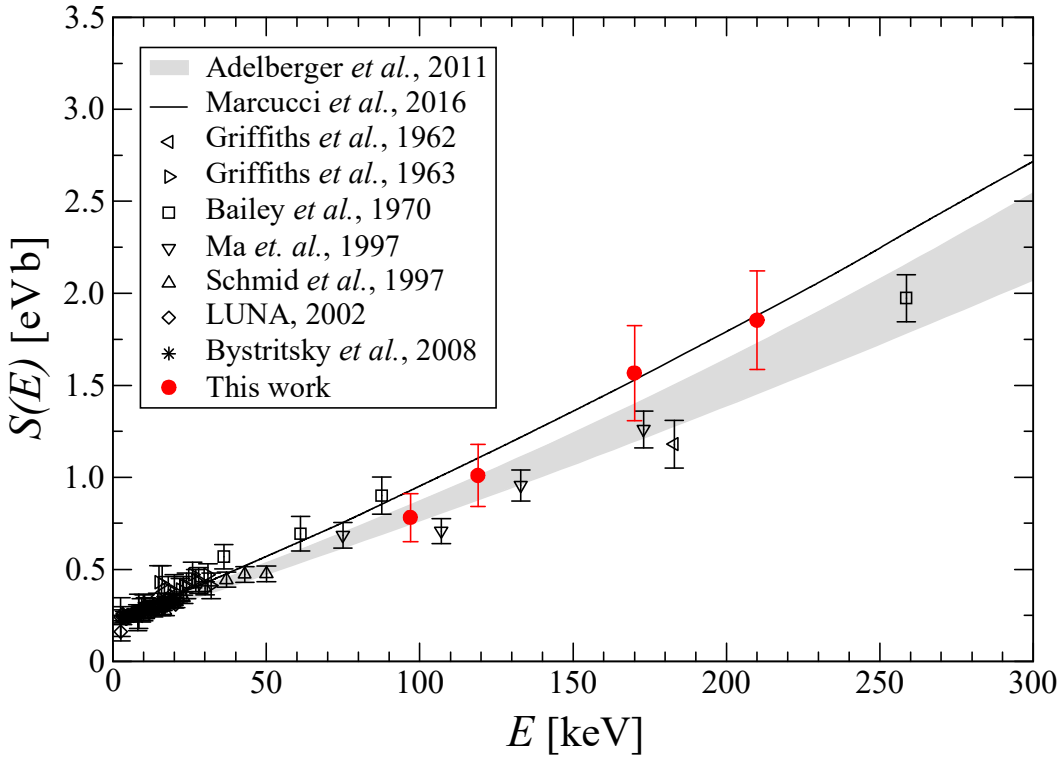

$$p + D \rightarrow {}^{3}He + \gamma$$

$$\sigma = \frac{S(E)}{E} \cdot e^{-2\pi\eta},$$

$e^{-2\pi\eta}$, Gamow penetrability factor

Sommerfeld parameter: $$\eta = \frac{Z_1 Z_2 e^2}{4\pi\varepsilon_0 \mathrm{h}c} \cdot \sqrt{\frac{\mu c^2}{2E}}$$

I. Tisma et al., Eur.Phys.J. A 55, 137 (2019)

Inverse kinematics

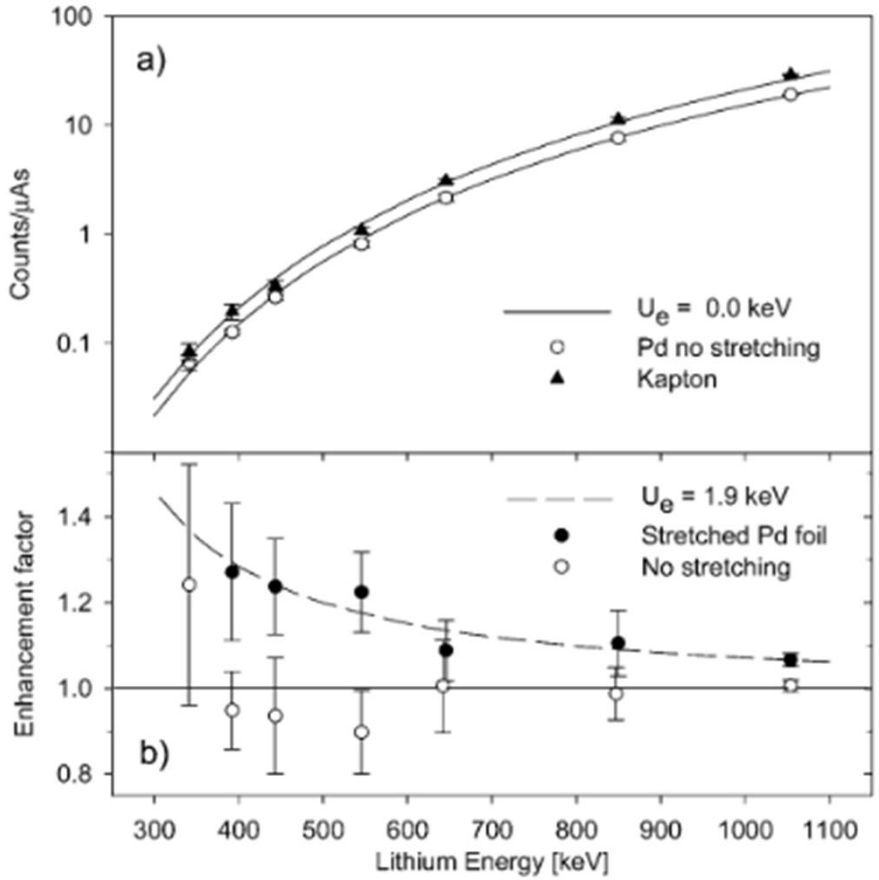

$^{1}H(^{7}Li,\alpha)^{4}He$

M. Lipoglavsek et al.,
Eur. Phys. J. A44, 71–75 (2010)

Thick Targets

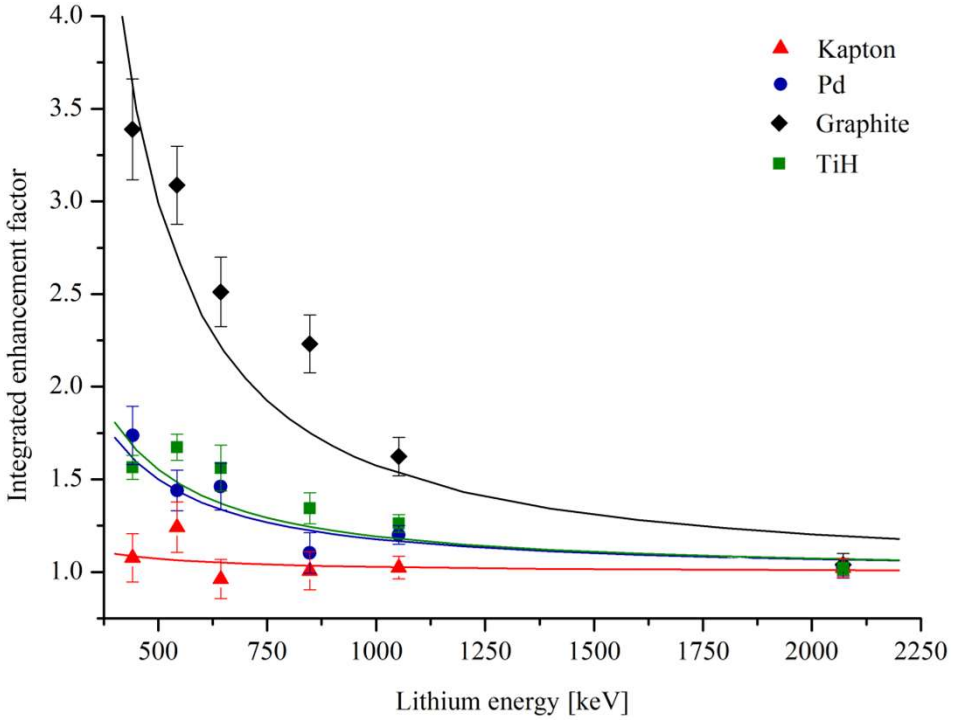

$^{1}H(^{7}Li,\alpha)^{4}He$

Target	U_e [keV]	Stoichiometry
Graphite	10.3 ± 0.4	0.059±0.003
Pd	3.6 ± 0.7	0.21±0.01
TiH	3.9 ± 0.4	1.03±0.04
W	5.9 ± 0.9	0.042±0.003

Adiabatic limit: U_e= 0.24 keV

Inverse Kinematics Fluorine

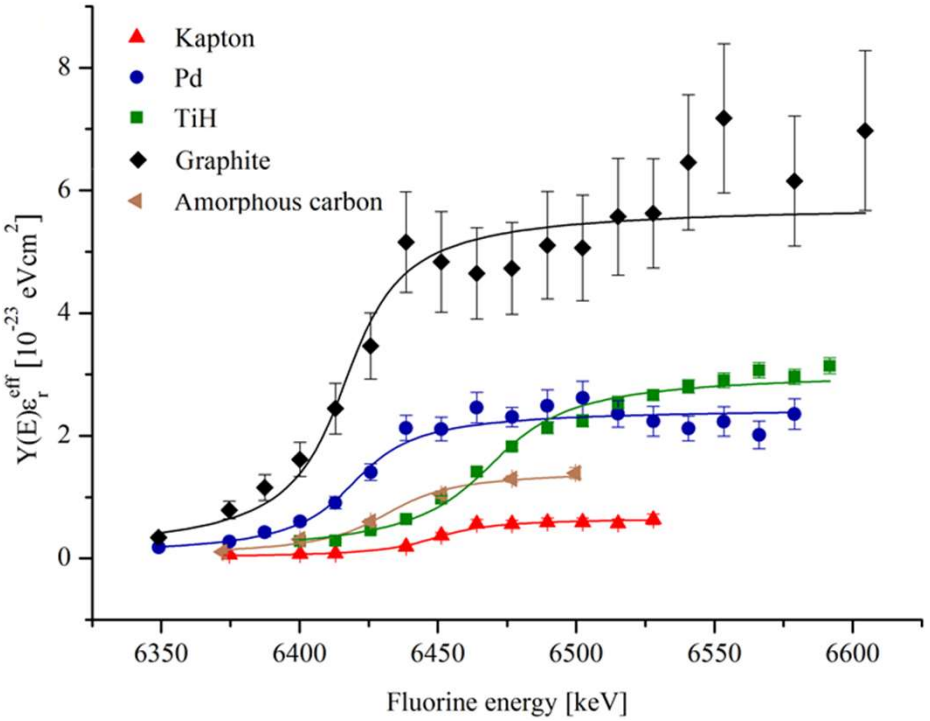

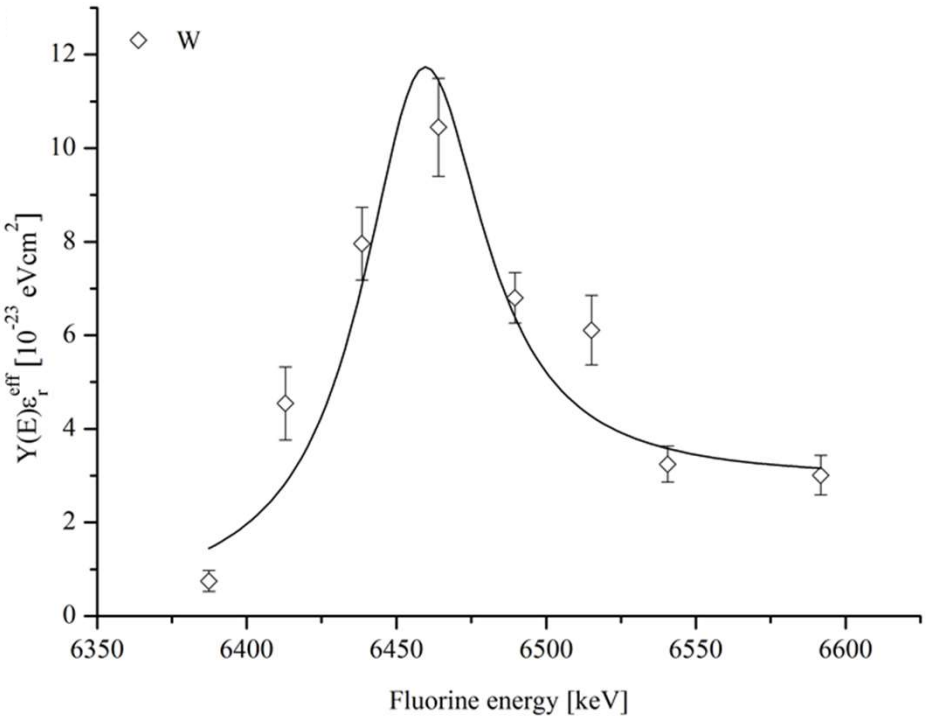

A. Cvetinović, PhD Thesis, University of Ljubljana (2015).

Results

Target	Reaction U_e [keV] ^{7}Li+p	^{11}B+p	^{19}F+p
adiabatic	0.24	0.68	2.19
Graphite	10.3 ± 0.4	32 ± 4	115 ± 8
Pd	3.6 ± 0.7	8.0 ± 1.9	63 ± 6
TiH	3.9 ± 0.4	6.7 ± 1.8	62 ± 6
W	5.9 ± 0.9	-	75 ± 15
Graphite/ adiabatic	42.9 ± 1.7	47.1 ± 5.9	52.5 ± 3.6

A. Cvetinović, Phys. Rev. C **92** (2015) 065801.

Inverse vs. normal kinematics

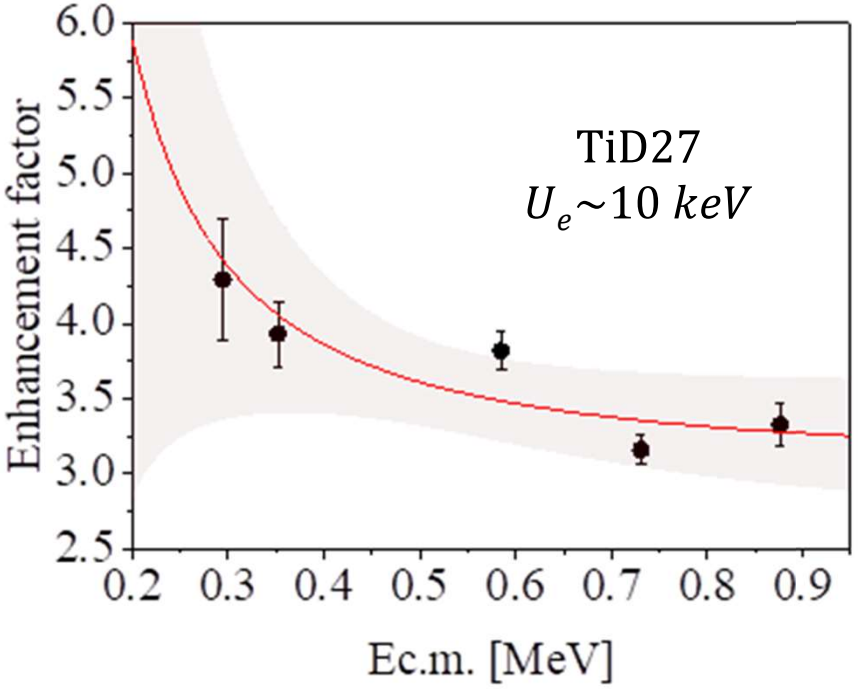

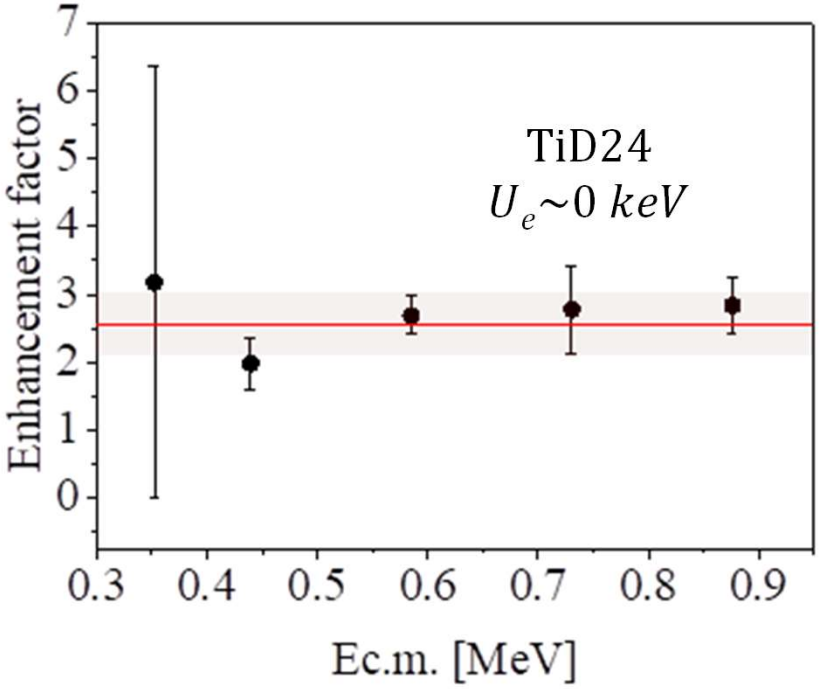

$TiD_{1.4}$ fully loaded

$TiD_{0.01}$ loaded and heated to 400˚C

Enhancement factor: $f = \frac{e^{-2\pi\eta(E+Ue)}}{e^{-2\pi\eta(E)}}$